# Water Safe Cities
## Technical Report

June 2022

C40 CITIES


# TABLE OF CONTENTS



C40 CITIES · POUL DUE JENSEN FOUNDATION · GRUNDFOS · Climate Adaptation Services · IVM Institute for Environmental Studies · VU

Photo @Jonathan Ford @Unsplash




# ACRONYMS

| | |
|---|---|
| CAS | Climate Adaptation Services |
| CWM | City water map |
| DA | Drought activity |
| DEM | Digital elevation model |
| EAI | Expected Annual Impact |
| FLOPROS | Flood Protection Standards |
| GCM | General circulation model |
| GDP | Gross domestic product |
| GHG | Greenhouse gas |
| GTSM | Global Tide and Surge Model |
| IPCC | Intergovernmental Panel on Climate Change |
| IVM | Institute for Environmental Studies |
| MERIT | Multi-Error-Removed Improved-Terrain |
| PBL | Netherlands Environmental Assessment Agency |
| PDSI | Palmer Drought Severity Index |
| RCP | Representative concentration pathway |
| SPEI | Standardized Precipitation and Evapotranspiration Index |
| SPI | Standardized Precipitation Index |
| SRI | Standardized Runoff Index |
| SSMI | Standardized Soil Moisture Index |
| SSP | Shared socio-economic pathway |
| UNDRR | United Nations Office for Disaster Risk Reduction |
| WASP | Weighted Anomaly of Standardized Precipitation |
| US | United States (of America) |


# 1. Introduction

Climate change, urbanisation and population growth are causing water availability and safety issues in cities around the world. Of all natural hazards, flood and drought affected the most people between 2000 and 2019. Around 1.65 billion people were impacted by floods and 1.43 billion by drought.[1] Whether it be too much water too quickly, with extreme rainfall resulting in flash flooding in urban areas,[2] or not enough water, because of long-term drought conditions,[3] no city is immune to these climatic changes. Sea-level rise and storm surges could force hundreds of millions of people in coastal cities from their homes at a total cost of more than US$ 1 trillion a year by 2050.[4] This increased migration and urbanisation is putting pressure on city water systems and infrastructure. Floods and droughts are, therefore, threatening the welfare of urban citizens and the critical services and operation of cities.

Cities and their leaders need to understand this complex and imminent threat and its consequences. Knowing how much flooding and drought a city will experience and the potential impacts of these hazards will prompt city authorities and financiers to take action on adaptation and resilience. To this end, the analysis behind Water-safe Cities report quantifies the future hazards of flooding and drought in 97 C40 cities by 2050 and the expected annual impact this will have on populations, urban infrastructure and the gross domestic product (GDP) of a city. The modelling and analysis have been used to develop interactive maps hosted on the Water-safe Cities webpage and the key headlines and messages of the research.

# 2.
# About this report

This Technical Report details the methodology developed by the Institute of Environmental Studies and Climate Adaptation Services, in collaboration with C40 Cities, of the key communication tools behind the project.

We first look to quantify the flood and drought hazard to C40 cities. Flood and drought risk are quantified in line with the common definition of risk as a function of hazard, exposure and vulnerability (see the Definitions section). Specifically, we assess three types of flooding (riverine, stormwater and coastal), as well as two types of drought (agricultural and hydrological). Because of data limitations, we have assessed stormwater flooding using the probability of extreme rainfall events as a proxy. To calculate the socio-economic impact for riverine and coastal flooding, we use state-of-the-art global flood risk models, taking into account future socio-economic scenarios and using shared socio-economic pathways (SSPs) based on land-use projections from the 2UP exposure model.[5]

We measure hydrological drought by estimating the annual deficits in urban water supply using modelled discharge time series and empirical extraction data. For agricultural drought, we assess modelled rootzone moisture shortfalls in agricultural areas around a city. After providing a socio-economic context for each city, we monetise the risks in US dollars for riverine and coastal flooding and hydrological drought using depth-damage curves and unit costs for water production/savings.

The analysis is divided into two parts:

**PART I**

A climate hazard analysis: populating our models with hydrological parameters to estimate the flood and drought hazard for 97 C40 cities.

**PART II**

A socio-economic risk analysis: combining hazard, exposure and vulnerability parameters to calculate socio-economic risk and the probabilistic impacts of flooding and drought.



# 3.
# How we define flooding and drought

Here, we define the climate hazards we used to produce our climate and socio-economic risk analyses and the interactive global maps.

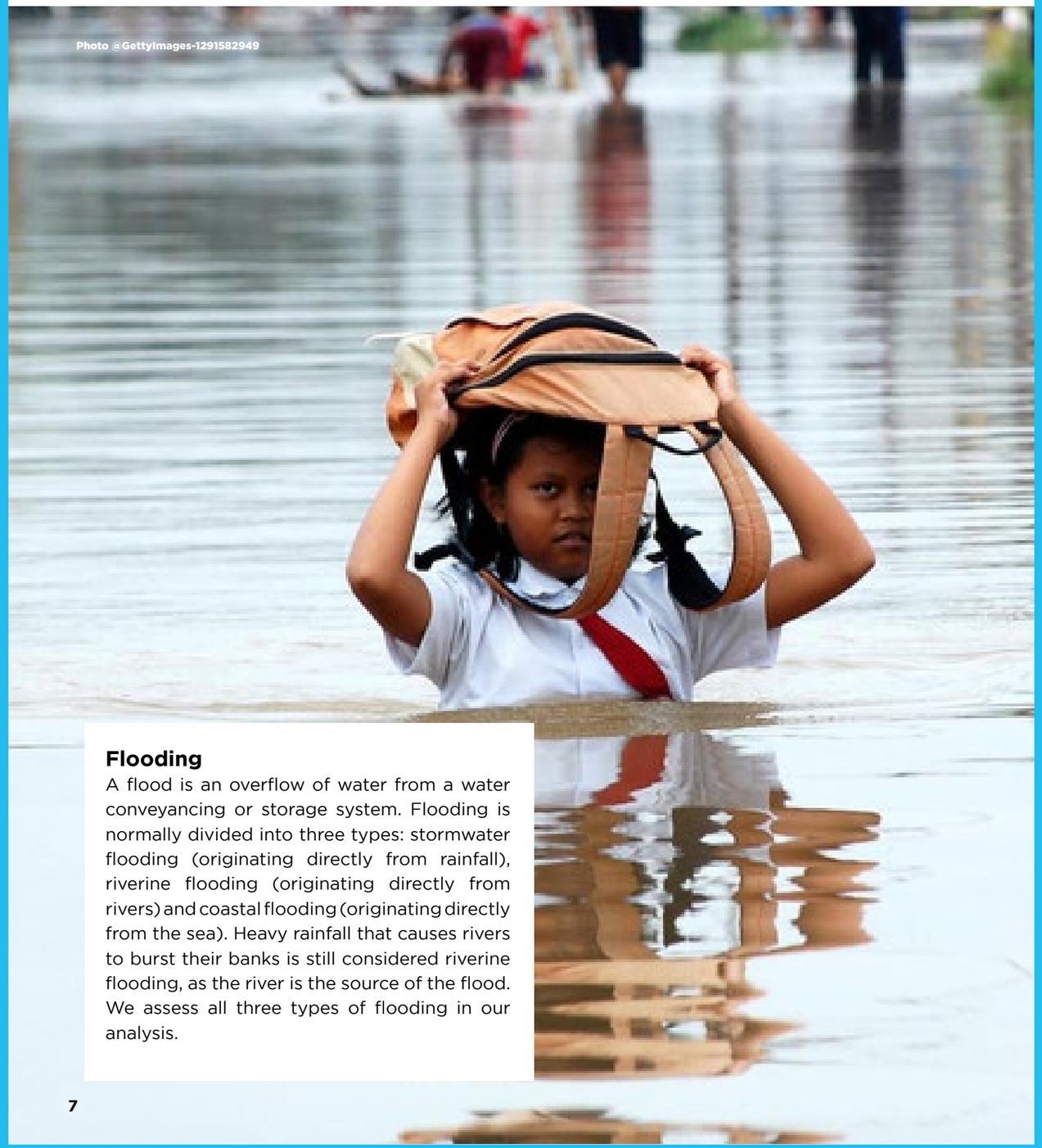
Photo @GettyImages-1291582949

## Flooding

A flood is an overflow of water from a water conveyancing or storage system. Flooding is normally divided into three types: stormwater flooding (originating directly from rainfall), riverine flooding (originating directly from rivers) and coastal flooding (originating directly from the sea). Heavy rainfall that causes rivers to burst their banks is still considered riverine flooding, as the river is the source of the flood. We assess all three types of flooding in our analysis.




Photo @Gyan Shahane @Unsplash

## Drought

A drought is essentially a temporal shortage of water relative to a climatic baseline or historical average.[6] However, water deficits can occur in different parts of the hydrological cycle, which makes a comprehensive definition challenging.[7] In addition, droughts are often slow and creeping in nature, which makes it hard to define their onset, duration and end.[8] It is also hard to delineate the spatial border of a drought, as it is not directly observable.[9] Consequently, scientists and policymakers have put forward a variety of alternative definitions in recent decades, sparking the creation of more than 150 drought indices. [10]

In recent decades, droughts have frequently been divided into three distinct types:

1. Meteorological drought – a shortage of rainfall.[11]
2. Agricultural drought – a shortage of soil moisture that would otherwise be available for crop and vegetation growth. [12]
3. Hydrological drought – a lack of (sub-) surface water, including streams/rivers and roundwater.[13]

Thus, an appropriate definition of drought depends on the stage of the hydrological cycle. This, in turn, comes down to the (expected) impacts a drought will have on the area in question.[14] In section 5.1, we assess the expected impacts of drought in urban areas and determine the type(s) of drought relevant to this project.

A different but related concept is that of water scarcity, which is excess water demand relative to supply for a certain economic activity. Water scarcity differs from drought in that it is considered a systemic state (something permanent or 'normal') rather than a temporary phenomenon.[15] This study will focus primarily on drought, as it is more directly climate related than water scarcity, based on the definitions used here. For a practical example of water scarcity and its impact on cities, please see our accompanying web narratives.
For detailed descriptions of how we define risk, please see the Definitions section.

# 4.
# Cities in this analysis

Below are the 97 C40 cities that are part of this research.

**Figure 1.** C40 cities

Abidjan
Accra
Addis Ababa
Amman
Amsterdam
Athens
Auckland
Austin
Bangkok
Barcelona
Beijing
Bengaluru
Berlin
Bogotá
Boston
Buenos Aires
Cape Town
Chengdu
Chennai
Chicago
Ciudad de México
Copenhagen
Curitiba
Dakar
Dalian
Dar es Salaam
Delhi NCT
Dhaka
Dubai
Durban
(eThekwini)
Ekurhuleni
Freetown
Fuzhou
Guadalajara
Guangzhou
Hangzhou
Hanoi
Heidelberg
Ho Chi Minh City
Hong Kong
Houston
Isanbul
Jaipur
Jakarta
Johannesburg
Karachi
Kolkata
Kuala Lumpur
Lagos
Lima
Lisbon
London
Los Angeles
Madrid
Medellin
Melbourne
Miami
Milan
Montreal
Moscow
Mumbai
Nairobi
Nanjing
New Orleans
New York City
Oslo
Paris
Philapelphia
Phoenix
Portland
Qingdao
Quezon City
Quito
Rio de Janeiro
Rome
Rotterdam
São Paulo
Salvador
San Francisco
Santiago
Seattle
Seoul
Shanghai
Shenzhen
Singapore
Stockholm
Sydney
Tel Aviv
Tokyo
Toronto
Tshwane
Vancouver
Venice
Warsaw
Washington D.C.
Wuhan
Yokohama
Zhenjiang



Photo @Sander Crombach @Unsplash

# 5. Methodology

Our overall methodology consists of the four steps outlined in Figure 2.

### 1. Populating our models

*Result:* daily hydrological parameters

### 2. Developing global hazard maps

*Result:* Estimation of hydrological hazards for flooding and drought

CLIMATE SCENARIOS

### 3. Calculating socio-economic impacts

*Result:* socio-economic impacts for flooding and drought, for different return periods

CLIMATE SCENARIOS SOCIO-ECONOMIC SCENARIOS

**PART I**

### 4. Estimating probabilistic risk

*Result:* average impacts per year (e.g. expected annual damage or affected people) for **97 C40 Cities**

CLIMATE SCENARIOS SOCIO-ECONOMIC SCENARIOS

**PART II**

Figure 2. Summary of the methodological approach

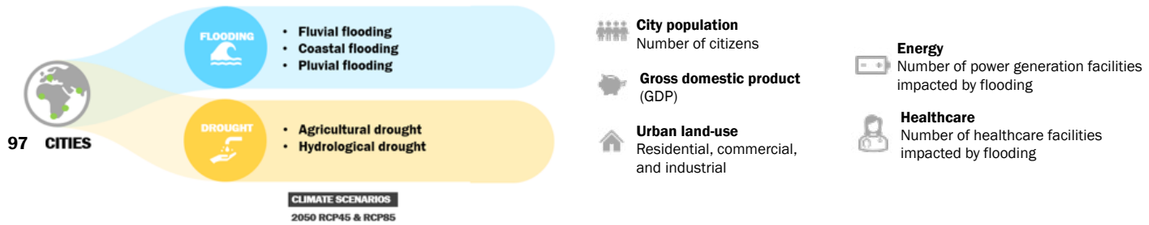




Photo @Saikiran Kesari @Unsplash

## 5.1
# Part I: Climate hazard analysis

For our climate hazard analysis, we review the first two steps in creating and populating global climate models to produce our global hazard maps.

### 1. Populating our models
*Result:* daily hydrological parameters

### 2. Developing global hazard maps
*Result:* Estimation of hydrological hazards for flooding and drought

CLIMATE SCENARIOS

**PART I**

Figure 2a. Summary of the methodological approach (Part I: Climate hazard analysis)

Any climate risk model requires comprehensive data and the integration of hazard, exposure and vulnerability parameters to achieve the best possible estimate of climate risk. In other words, the more detailed the input information on these factors, the closer the estimate will be to reality. Furthermore, a distinction is often made between models and studies that simulate only the climate risk of the current situation and those that estimate the climate risk of future scenarios. In our methodology, hazard, exposure and vulnerability can be statically (unable to evolve over time) or dynamically (able to evolve over time) added to the model. [16]

To make predictions, climate risk assessments often make use of representative concentration pathways (RCPs)[17] for scenarios on future greenhouse gas (GHG) concentrations and SSPs for scenarios on socio-economic development. RCPs and historical data on GHG concentrations are used in general circulation models (GCMs). A GCM models the climatic state of the earth based on a set of boundary conditions (mainly solar radiation and GHG concentration). The output of a GCM (for example, atmospheric temperature or rainfall) is also the input for hydrological models, which use this data to simulate hydrological processes, resulting in runoff/streamflow and groundwater recharge.

Next, the magnitudes and corresponding probabilities of possible hazardous events can be extracted. The probability of a hazardous event happening is often expressed in conjunction with a 'return period', especially in the case of flooding. This is the average amount of time (usually in years) between two such events. It is more precisely defined as the inverse of the probability that an event is exceeded in any one year: Rp = 1/P.


Photo @Tebogo Losaba @Unsplash



**Understanding return periods**

Return periods are often determined using extreme value analysis. This involves conducting an assessment based on past events above a certain threshold or the maxima/minima each year. This series of events is ranked from the most extreme to the most common, then a statistical (extreme value) distribution is fitted to the data. From this fit, it is possible to derive the expected magnitude of an event for each return period. It is also possible to extrapolate this when acknowledging the uncertainty of exceeding known events. Hence, a 10,000-year event can be estimated without ever being observed, albeit with a high uncertainty interval.

Rp is the return period in years and P is the probability of an event being exceeded in any one year (exceedance probability). For example, if a flood of volume X happens statistically once every 100 years, the return period of that flood is said to be 100 years. The probability of a flood of at least that magnitude occurring in a given year becomes (1/100)*100% = 1% a year. Obviously, these return periods tend to be based on historical data; the exact statistical probability of any hazardous event occurring is unknown. This also means that a 100-year event might not occur in the next 100 years or that a 100-year event might occur several times in 100 years. For instance, high water levels and consequent flooding happened along the Rhine and Meuse rivers in both 1993 and 1995. Statistically, these events were estimated to occur only once every 25-50 years. [18]

Note: We use return periods in this study to indicate the probability of flooding, but do not use them in our drought risk assessment.

It should be stressed that return periods are dynamic, so evolve over time. A return period is linked to a certain magnitude of event. If, due to climate change, events of this magnitude happen more frequently, their return period will decline. For example, a 10-year return period rainfall event might equal a downpour of 40mm/hour in a certain city. Hence, every year, there is a (1/10)*100% = 10% chance that this will happen. Should precipitation patterns change due to climate change and that 40mm/hour event now have a 20% probability of occurring per year, this would alter the return period to 1/(20%/100%) = 5 years. Thus, the return period for the event would halve because the frequency of the event had doubled due to climate change.

Another general assumption is that the Global Human Settlement Model Grid (GHS-SMOD) city border dataset is the most suitable dataset for global flood and drought assessments. Countries define their cities in different ways,[19] which makes it difficult to consistently compare urban flood and drought risk between countries. This can be overcome by choosing a physical definition for cities rather than an administrative one.[20] The GHS-SMOD applies such a definition and bases it on building and population density thresholds,[21] making it consistent between countries.[22] However, a physical definition also means that adjacent cities can be merged into one agglomeration within the dataset. Still, it is likely that impacts in one city will spill into adjacent cities, as they are probably economically connected.

## Step 1:
# Populating our models

For this study, we use data from the PCRaster GLOBal Water Balance model (PCR-GLOBWB)[23] as the basis for simulating river flooding and the water supply side for hydrological drought. In this study, we used the new version of the model from 2018.[24] PCR-GLOBWB is a global hydrological model that simulates daily hydrological parameters such as discharge and the water volume that resides in the floodplains of rivers at a resolution of 5' x 5' (around 10 km x 10 km at the equator).

The output of the climate model is used directly or indirectly to calculate hazard indicators. For our purposes, indirectly means that a global hydrological model is used to calculate the corresponding values of discharge and rootzone moisture (the volume of moisture in the top 1 metre of the soil) from these climate model outputs. These values are then inserted into another model that calculates the hazard.

**Riverine flooding**
For riverine flooding, PCR-GLOBWB overbank flow volumes are used to develop inundation maps using the mass-conservative flooding algorithm developed by Winsemius et al. (2013). We use this to generate global maps showing the extent and depth of flooding for different flood return periods (2-, 5-, 10-, 25-, 50-, 100-, 250-, 500- and 1,000-year return periods) at a horizontal resolution of 30" x 30" (around 1 km x 1 km at the equator).

**Coastal flooding**
We model coastal flooding by (a) modelling the sea level for different return periods and (b) simulating the on-land inundation from these sea levels. The sea level comprises three components: the tide, the storm surge and wind waves. We do not include the latter here. For step (a), we use the Global Tide and Surge Model (GTSM) to simulate the sea levels resulting from storm surge and tide for the return periods as described for riverine flooding. We use the latest version of GTSM.[25] The model resolution is 2.5 km from the coast (1.25 km in Europe). GTSM is forced with ERA5 high-resolution meteorological forcing data.[25] This dataset has a spatial resolution of 30 km x 30 km, enabling it to better resolve tropical cyclones than earlier versions of GTSM.[26] The baseline period for these simulations is 1979-2017 (for climate forcing), with a mean sea level equivalent to the 1986-2005 period. For future simulations, probabilistic sea-level rise projections were carried out using the method presented by Le Bars et al. (2017), based on CMIP5 data for RCP 4.5 and RCP 8.5.

Next, in step (b), the extreme sea levels for different return periods are converted into flood hazard maps using the approach described in Tiggeloven et al. (2020). This approach uses a GIS-based routine, in which the GTSM extreme sea levels are projected to the nearest coastline, with inundation taking place in areas that are hydrologically connected to the sea at that extreme sea level. The model uses the Multi-Error-Removed Improved-Terrain (MERIT) Digital Elevation Model as underlying topography (30" x 30") and we use a resistance factor to simulate the inward reduction of flooding land, as tides and storm surges have a limited timespan.

**Stormwater flooding**
For stormwater flooding, to represent the future hazard, we use daily rainfall data that come directly from GCMs.[26] We used rainfall data from ISIMIP2b for the following GCMs: GFDL-ESM2M, HadGEM2-ES, IPSL-CM5A-LR, and MIROC5, again for RCPs 4.5 and 8.5.

## DROUGHT

Because of their complexity and diversity, it is often difficult to find a comprehensive set of indicators for drought risk. This has led to a variety of approaches and datasets in global drought risk assessment. Most drought indices focus on rural rather than urban areas, and drought risks to or impacts on cities are investigated more often on a local or regional scale.[27] Moreover, drought risk damages have not been widely monetised on a global scale before.[28]

As mentioned, there is no single, comprehensive drought indicator. Whether a given indicator is relevant to this assessment depends on the water sources affected by drought and whether this has an impact on cities. We, therefore, gathered information on drought impacts in urban areas



to determine which parts of the hydrological cycle were relevant. We then chose two drought indicators for this assessment: hydrological drought and agricultural drought. We elaborate on this process of indicator selection below, based on their impacts on urban areas.

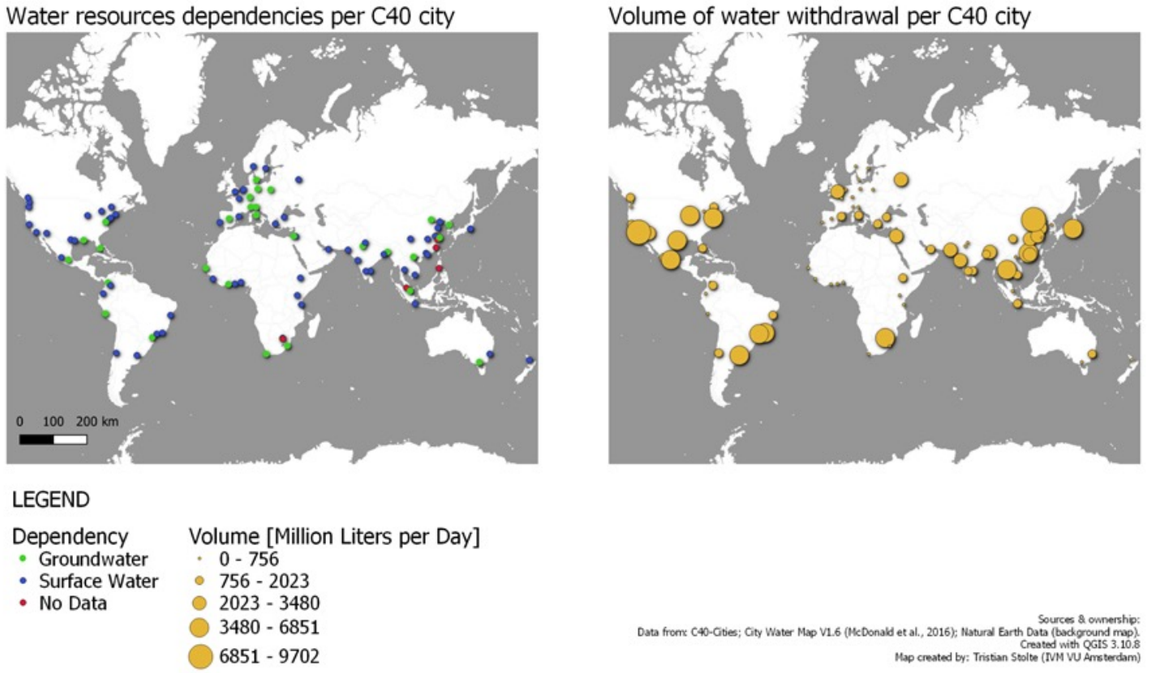


Figure 3.
Left: Water resource dependency per C40 city, according to the City Water Map database (CWM)[29]

**Urban water sources**
Drought impacts in cities are most often related to urban water supply and agricultural practices. To assess shortfalls in urban water supply (domestic and industrial), it is important to identify the source of this water. McDonald et al. (2014; 2016) created a dataset in which they showed the municipal water sources for 534 large urban agglomerations (with a population of more than 750,000) globally. This dataset also includes the source type (for example, surface water or groundwater), as well as an estimate of the volume of water withdrawals for several agglomerations. According to this dataset, cities most often depend on either groundwater or surface water. A city is deemed reliant on a specific source if 50% or more of its water originates from that source. Sporadically, other water sources (such as desalination) are used, but these do not meet the 50%-plus criterion for any city. Moreover, saltwater bodies are generally too large to be affected by drought and hinder desalination. Hence, a drought in surface water or groundwater is likely to have the greatest impact on an urban area in terms of public water supply. This is what is called a hydrological drought. The water dependency of the C40 cities can be found in Figure 3 (spatially) and Table 1 (overview).

Right: Volume of water withdrawals per C40 city, according to the CWM

**SELECTING INDICATORS**
Establishing two main categories of drought impact in urban areas calls for two different drought indices, each able to estimate the drought hazard for one of those categories.

Spatially standardised indices are often preferred for studies on a global scale because:

- They allow a comparison of values between different climatic zones.
- They require fewer data points.
- Their interpretation is intuitive.
- They perform robustly over multiple studies.

This type of indicator is especially useful when no absolute threshold is known beforehand. The threshold below which drought occurs will then be based on local climatic conditions and the corresponding statistical occurrence of dryer-than-normal events.

| Dependent on | Percentage of C40 cities |
|---|---|
| Surface water | 63% |
| Groundwater | 18% |
| No estimate | 14% |
| Not in database | 5% |

Table 1. Water-source dependency of C40 cities (surface water and groundwater)

Note: Not all 97 cities are included in the water resources database and there are cities without estimates for water withdrawal volumes. An alternative methodology for classifying hydrological drought from a qualitative methodology methodology in Annex 2.

**HYDROLOGICAL DROUGHT**

We came up with a non-standardised indicator for the urban water supply in this study as it enabled an absolute threshold to be derived for each water source. This indicator compares water availability (water supply) from the hydrological model with estimates of daily water withdrawals (water demand) per water utility. The latter were found in the CWM database,[31] which contains the locations of water utilities for at least 88 of the 97 C40 cities.

**Because of uncertainties and missing data, to link the withdrawal data to water availability, we had to make four assumptions:**

- **The first states that all the water extracted has a specific (economic) purpose and that no water is stored. The drought impact might be lessened in reality if water were either stored or preserved as a buffer against drier periods.**
- **The second is that water withdrawals are proportionally linked to discharge at the withdrawal location. Again, it is likely that some water is saved or not extracted as a buffer under normal conditions, so that not every deviation from the mean instantly leads to drought. Therefore, the relationship is probably less elastic; if discharge drops by 10%, water extraction may drop by less than 10%.**
- **The third is that the total surface water shortage will be equally distributed among the citizens of the city affected by drought. However, the poor and other socio-economically disadvantaged citizens are likely to be hit harder by the drought than the generally more resilient, richer population.**
- **The fourth is that groundwater is sustainably extracted. Groundwater extractions are not taken into account here. On the one hand, they could alleviate parts of the hydrological drought by serving as an alternative to surface water sources. On the other, they could worsen the drought when groundwater is unsustainably extracted and when drought hits those sources as well. The latter is a likely scenario, as groundwater and surface-water deficits are both embodiments of a hydrological drought, so could occur at the same time. For the cities, it also depends on the location of their water sources. A groundwater source might be in another (part of a) watershed to the surface water source, so may not experience the same hydrological circumstances.**

**Furthermore, drought volumes are standardised per 1,000 inhabitants. Population counts are also extracted from McDonald et al. (2016). Thus, the hydrological drought hazard indicator is the expected annual volume of drought per 1,000 inhabitants.**

However, there are only withdrawal estimates for 76 of the cities.  estimates of daily water withdrawals (water demand) per water utility. The latter were found in the CWM database,[31] which contains the locations of water utilities for at least 88 of the 97 C40 cities. However, there are only withdrawal estimates for 76 of the cities. Where we were not able to account for the remaining C40 cities we have provided a qualitative methodology in Annex 2.

Furthermore, drought volumes are standardised per 1,000 inhabitants. Population counts are also extracted from McDonald et al. (2016). Thus, the hydrological drought hazard indicator is the expected annual volume of drought per 1,000 inhabitants.

**AGRICULTURAL DROUGHT**

The second main impact category is agriculture, which is caracterized by two drought types, depending on which irrigation strategy is chosen: either soil moisture drought for rainfed agriculture or hydrological drought for artificially irrigated agriculture.

Agricultural drought has been selected due to its indirect impact on urban areas. Furthermore, agricultural drought has been used to supplement our hydrological drought analysis as it was not possible to undertake a complete analysis for several C40 cities.

We use the Standardized Soil Moisture Index (SSMI) to assess agricultural drought, as it relates to rainfed agriculture, the most common type of agriculture.[33] The SSMI calculates the statistical distribution of soil moisture volumes for each month in a given year based on time series of soil moisture for that month. A threshold of -1 standard deviation is used, which means that if soil moisture drops below one standard deviation of the mean value, we consider it a drought. is the expected annual volume of drought per unit of area.

## Step 2:
# Developing global hazard maps

We use the aforementioned hydrological and climate parameters to develop the indicators of flood and drought hazards mentioned. These, in turn, provide hazard information for the 97 C40 cities. This section describes the development of each hazard map individually. Table 2 summarises the hazards and indicators used. To understand the resolution of each hazard map, please refer to the Resolution Tables in Annex 4.

### Flooding

On a global scale, the flood hazard for a certain geographical area is generally represented by the inundation depth and extent corresponding to a specific return period (see Understanding return periods on page 9). In the case of riverine flooding, the inundation depth and extent are derived from the spatial propagation of water from the overbank flow corresponding to the relevant return period. For each pixel on the gridded inundation maps, we multiplied the inundation depth by the area of that pixel (the extent) to get the inundation volume per pixel. The total inundation depth is the sum of all pixel volumes inside the city. We then standardise this by dividing by the total city area to obtain the hazard indicator for riverine flooding in terms of volume per area. We use the same process to derive the coastal flooding hazard, except that the flood water comes from the overtopping of coastlines rather than riverbanks.

The same approach cannot be used for stormwater flooding, as the model is not yet able to create global inundation maps for rainfall. Therefore, the change in extreme precipitation events per pixel is used as a proxy for future stormwater flooding hazard. The precise indicator is the factor change in the frequency of occurrence of a current precipitation event with a 10-year return period. For example, if a 10-year return period rainfall event of 40mm per hour becomes a five-year return period event in future, the hazard indicator takes on a value of 2, as the event becomes twice as frequent.

#### Riverine and coastal flooding

For riverine flooding, we produced hazard maps of the flood volume (the extent of the flood multiplied by the depth of inundation) for each city for different return periods, as described in section 5.3.




We took an ensemble mean of flood volumes per pixel, or the average flood volume for all GCMs. Next, we aggregated the flood volumes per city and standardised them to $m^3/km^3$ for comparable results between cities. This gave us an estimate of the riverine flooding hazard per city for each return period and climate scenario (that is, historical/current, RCP 4.5 and RCP 8.5).

We derived the coastal flooding hazard map in a similar way, giving us an estimate of the coastal flood hazard in $m^3/km^3$ for each combination of city, return period and climate scenario. The only difference is that coastal flood inundation maps are based on probabilistic sea-level rise projections, so are not calculated for different GCMs, but already statistically aggregated over different climate models.

For the surface area, we delineated each city using the city borders from the GHS-SMOD.[34]

In this study, we used a state-of-the-art method for our riverine and coastal flood assessments. The main limitations stem from the trade-offs in data availability and accuracy needed for global model analyses. We explain them further here, based on the work of Ward et al. (2020b) and Tiggeloven et al. (2020). The flood hazard modelling approach uses generic return-period maps, so does not consider specific flood events. This means, for instance, that a 1-in-100 event could correspond to different flood volumes in different parts of a city - and this is likely to be the case in reality. Moreover, the flood inundation simulations do not use a hydrodynamic modelling scheme and are carried out at a spatial resolution of 30” x 30”, which is not sufficiently granular to include local topographical features in cities.

Another limitation is that coastal and riverine flooding are considered independently of each other. This means, for instance, that the flood hazard simulations do not include downstream backwater effects in coastal cities. We, therefore, assume that rivers in coastal regions can flow away into the ocean without being impeded by high coastal water levels in deltas and estuaries (for example, caused by storm surge and high tide). The exposure data have a resolution of 30” x 30” and do not differentiate between different kinds of urban fabric. However, we have made an estimate of the percentage split of urban area between residential and commercial and industrial land use. Also, standard depth-damage functions are used around the globe due to a lack of spatially disaggregated information. These curves only apply to direct damages and exclude indirect damages.

#### Stormwater flooding

For stormwater flooding, we calculated changes in the occurrence of extreme rainfall events. We chose the current 10-year return period event as our baseline and calculated how much the frequency of this event might change in future scenarios. As mentioned, return periods are dynamic. For each pixel inside a city, we took the total time series of daily rainfall from the historical data (1971-2006). For each year, we looked for the maximum rainfall volume per day and then sorted those maximum levels from large to small. We then searched for the 10-year return period rainfall event and identified the corresponding rainfall volume.

We performed the same sorting process on the future scenario data (2030-70) and identified the rainfall volume of the historical/current 10-year return period event in the future time series. We then calculated the corresponding future return period and divided it by the historical return period to obtain the change in frequency of occurrence. We then averaged these numbers over all climate models and all pixels inside a city to get an estimate of the stormwater flooding hazard per city per RCP. Cities were again delineated using GHS-SMOD.

As mentioned, there is a big data challenge in assessing stormwater flooding on a global scale. This means we could only provide a simple proxy for the stormwater flood hazard here. Consequently, we have not estimated the damage from stormwater flooding. Nonetheless, the hazard maps highlight several cities as potential hotspots of stormwater flood risk, and this could be an incentive for more detailed studies on those cities.

Furthermore, we have analysed the change in frequency of a 10-year rainfall event rather than the change in volume, as the non-granular resolution of the input data did not allow us to accurately estimate total rainfall volumes at city level. Hence, the change in frequency is probably more consistent over different spatial scales than the change in volume. The 10-year event itself was chosen based on the temporal resolution (daily) and temporal extent (35-40 years) of the input data. Higher-intensity events require longer time series, as they occur less often than lower-intensity events.

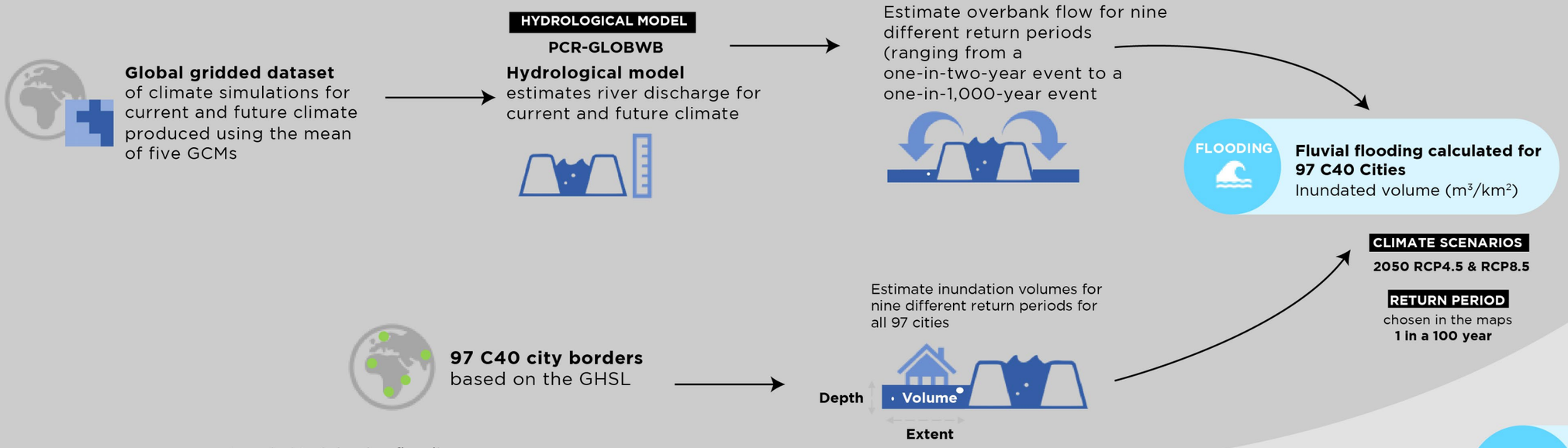


Figure 4a. Visual summary of the methodology behind riverine flooding

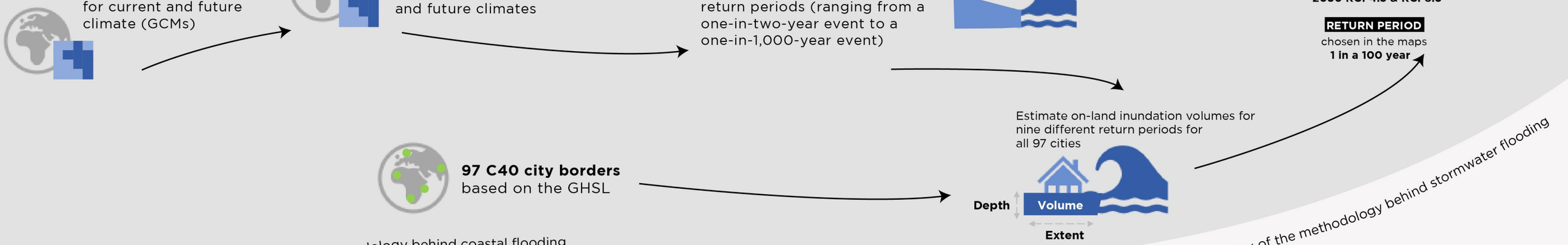


Figure 4b. Visual summary of the methodology behind coastal flooding

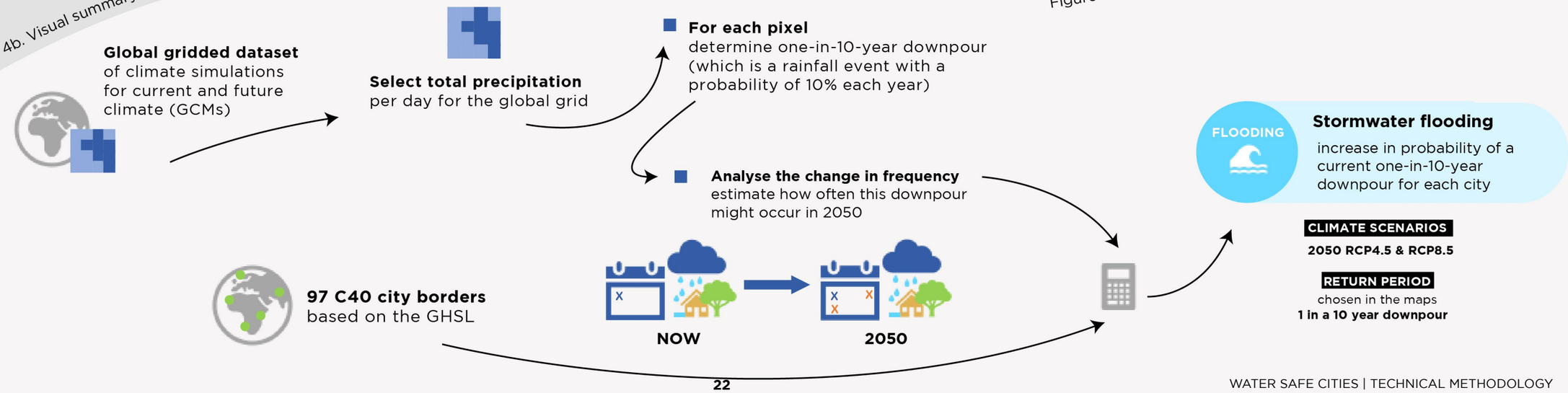


Figure 4c. Visual summary of the methodology behind stormwater flooding

**Hydrological drought**

For hydrological drought, we created a time series of discharge per calendar month and calculated the average discharge per pixel for each month in the series. This resulted in 12 average discharge values per pixel, one for each month of the year. We then analysed the complete discharge time series and identified when the discharge was below average for the corresponding month. We assumed that shortages occurred below this threshold. We then added up the annual water shortages per city surface water source and per city. Note that several cities extract their water from multiple surface water sources. Next, we averaged the total water shortages per city per year over the climate models and divided this by the number of city inhabitants. This hazard is thus expressed per 1,000 inhabitants per city per RCP. Note, too, that this metric inherently includes exposure by considering the number of citizens. We used only the CWM population counts for the 2010 base year to separate out the climate effects on future changes in drought hazard.

In summary, the main assumptions used in our hydrological drought hazard calculations likely lead to an overestimate of actual drought volumes from surface water. These could be either alleviated or aggravated by drought volumes that originate from groundwater sources. Moreover, these drought volumes potentially hit poor citizens harder than wealthier ones; we have not been able to account for this in our analysis.

In addition, we also assume that cities use the water sources set out in the CWM database.[35] Unfortunately, not all C40 cities are included in the database and the information is incomplete for some cities. For example, Cape Town uses several surface-water sources for its water supply,[36] but these are not present in the CWM. Still, the database is the most complete overview of water withdrawals available on a global scale. For missing cities, we have provided a qualitative analysis and ranked their risk of hydrological drought below. A detailed summary of how this qualitative analysis was conducted can be found in Annex 3.

| Lower range | Upper range | Risk | Cities |
|---|---|---|---|
| **33%** | **<46.5%** | **Low** | None |
| **46.5%** | **<60%** | **Medium-low** | Zhenjiang, Hangzhou, Shenzhen |
| **60%** | **<73.5%** | **Medium** | Berlin, Fuzhou, Rome, Madrid, Dubai, Kuala Lumpur, Milan, Singapore, Medellín, Stockholm, Abidjan, Quezon City, Ekurhuleni, Jaipur, Miami |
| **73.5%** | **<87%** | **Medium-high** | Lima, Accra, Beijing, Curitiba, Delhi, Jakarta, Nairobi, New York, Shanghai, Washington, D.C., Johannesburg, London, Sydney, Cape Town, Melbourne, Rio, Copenhagen, Hanoi, Durban (eThekwini), Seoul |
| **87%** | **100%** | **High** | Los Angeles, Santiago, New Orleans |

Table 2. Hydrological drought risk analysis for C40 cities



**Agricultural drought**

For agricultural drought, we first used the SSMI to analyse time series of historical rootzone moisture and derive a standard normal distribution of rootzone moisture values per calendar month per grid cell. We identified a -1 standard deviation of historical rootzone moisture volumes for each grid cell, which we then translated back into an absolute volume of water. We assumed that there was a crop-damaging drought event if this threshold was exceeded, both in historical and future time series. We added up the total annual volume of water below the threshold for each grid cell. We then aggregated this information into one or more water provinces for each city, assuming that each city obtained its food from the water province(s) in which it was located. We also used physical agricultural area estimates from the MapSpam project to correct for the percentage of agricultural area in each water province. The last step in deriving the drought hazard for agricultural areas was to divide by the total surface area of the intersecting water provinces for each city. As we took the ensemble mean once again, the hazard was thus defined as the agricultural drought per city per climate scenario. As with urban water supply, we included exposure by defining the areas where potential damage could occur, namely, agricultural fields and the cities to which they belonged. However, we did not directly include the exposed elements in the cities themselves (for example, population or companies affected), as this information could not be ascertained from the data in hand.

In general, drought is very difficult to frame, especially on a global scale, so assumptions are required to quantify drought risk. In calculating occurrences of drought, a -1 standard deviation of historical rootzone moisture volume for each grid cell is assumed to be a crop-damaging drought event if this threshold is exceeded in either historical or future time series.

Another key assumption is that crop failure in a water province surrounding a city has an impact on the city's food supply and corresponding food prices. The import and export of food is not considered here due to data constraints, but it is likely that a city is not fully dependent on the farmlands in its own water province. However, even if crop failure in a region does not lead to food shortages in nearby cities, that region is still likely to suffer from local economic problems that may have chain effects for cities (for example, through food distribution and processing). Hence, this assumption does not, in and of itself, overestimate the drought costs for a city.

If a water province is shared by two or more cities, the drought hazard from that water province is shared equally between them. In reality, some cities may depend more heavily than others on the crops in a water province, so will experience a greater share of the total drought risk. Similarly, all crops are assumed to be equally affected by drought, although some may be more resistant than others. This means that some cities that depend on drought-resistant crops will experience a lesser drought impact than others. Moreover, the spatial resolution of 30 x 30 is not sufficiently granular to resolve agricultural droughts in very small water provinces.

On a technical note, the SSMI-based drought threshold is only calculated for those pixels that have at least 80% of the timesteps in the data. This cut-off point was chosen to exclude thresholds defined on just a few data points. The 80% is a somewhat arbitrary number based on the authors' expert judgement. Furthermore, the SSMI threshold was set at -1, which detects a moderate drought or worse according to Komesku (1999) or a moderate to severe drought according to the classification of Agnew (2000). The one-month lag time was chosen based on the assumption that cities needed to deal with drought immediately when it occurred and that no water was stored or saved in between. Moreover, if we used a larger time lag when calculating the annual deficit, this would result in double counting.

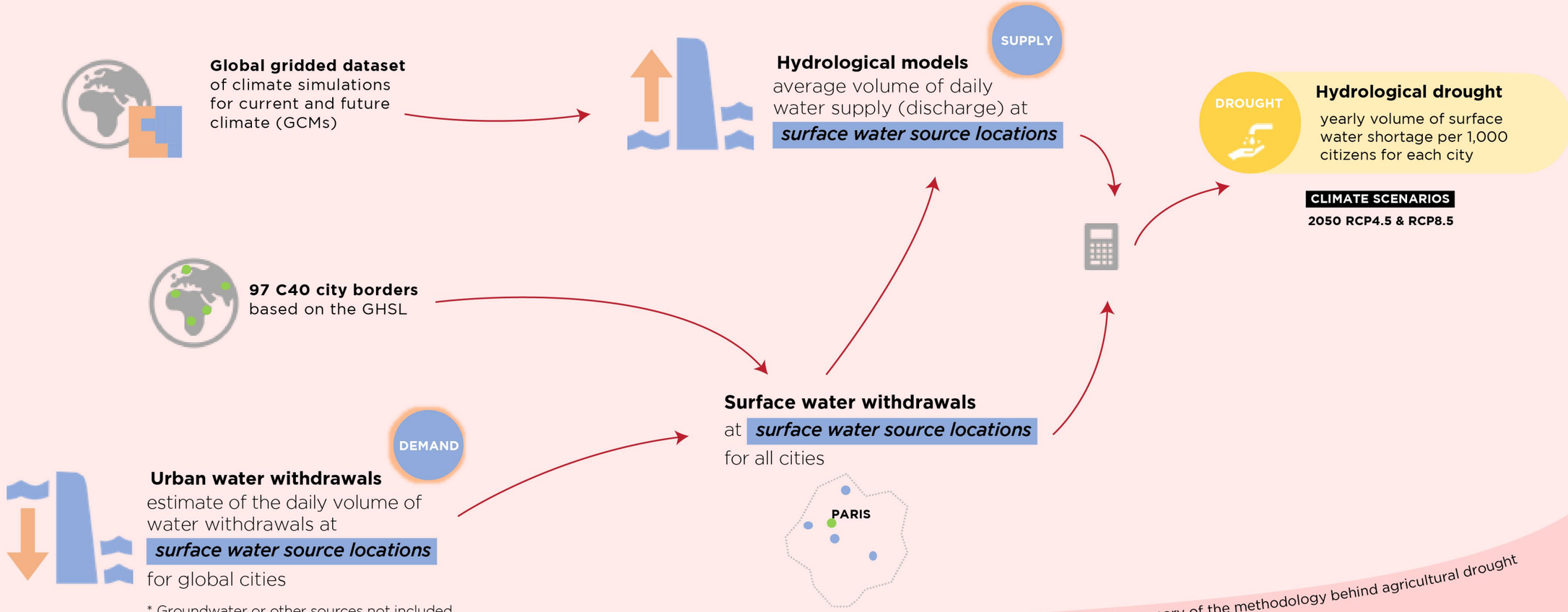


Figure 5b. Visual summary of the methodology behind agricultural drought

Figure 5a. Visual summary of the methodology behind hydrological drought

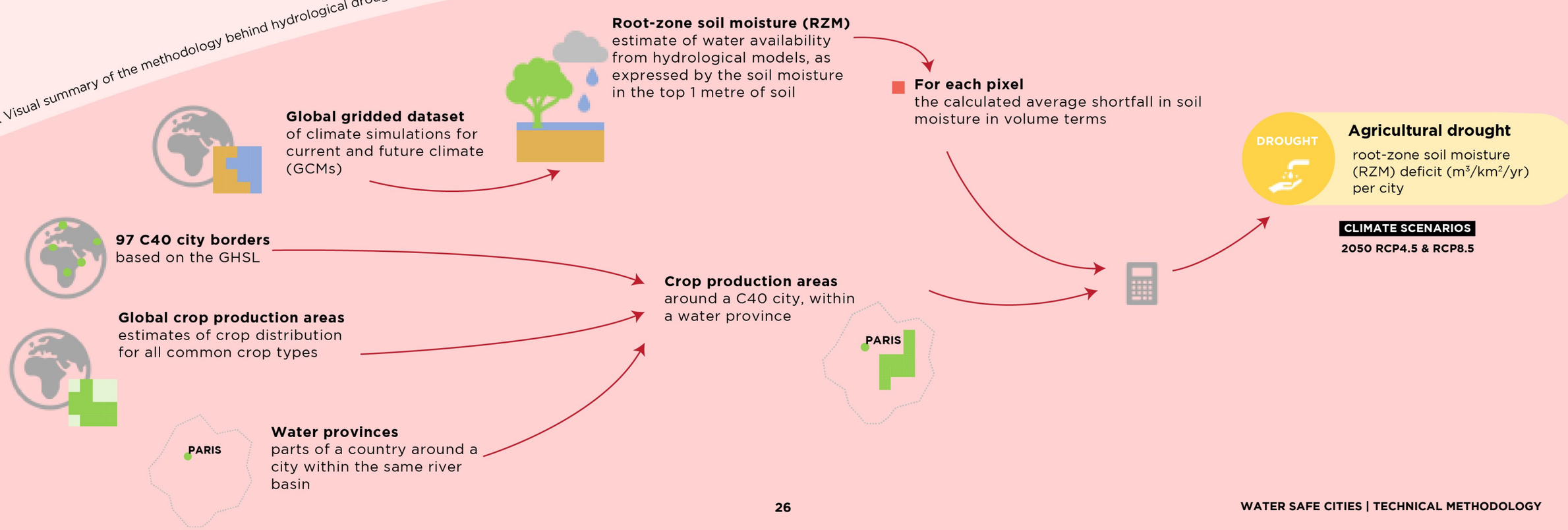

Photo @GettyImages-521341146

## Summarising our climate hazard analysis

The table summarises the climate hazards analysed in this research and the indicators used for each hazard, as well as the unit in which we produced results, as displayed in the Water-safe Cities interactive maps.

| Hazard | Indicator | Climate model ensemble | Spatial scale | Unit |
|---|---|---|---|---|
| **Riverine flooding** | Total flood volume | Yes, averaged | Per city | $m_3/km_2$ |
| **Coastal flooding** | Total flood volume | Yes, inherently included | Per city | $m_3/km_2$ |
| **Stormwater flooding** | Change in the frequency of a one-in-10-year precipitation event | Yes, averaged | Per city | factor of change; dimensionless |
| **Hydrological drought** | Urban water supply shortage | Yes, averaged | Per city (per inhabitant) | $m_3$/year/1000 inhabitants |
| **Agricultural drought** | SSMI | Yes, averaged | Per water province | $m_3/km_2$/year |

**Table 3.** Summary table of the climate hazards analysed and indicators used



## 5.2.
## Part II: Socio-economic risk analysis

The global hazard modelling methodology described in section 5.1., *Part I: Climate hazard analysis* provides the basis for *Part II: Socio-economic risk analyses*, in which we model the impacts and risks. We explain the methodology behind Part II later in this chapter.

**3. Calculating socio-economic impacts**

Result: Socio-economic impacts for flooding and drought for different return periods

CLIMATE SCENARIOS | SOCIO-ECONOMIC SCENARIOS

**4. Estimating probabilistic risk**

Result: Average impact per year (for example, expected annual damage and people affected) for **97 C40 Cities**

CLIMATE SCENARIOS | SOCIO-ECONOMIC SCENARIOS

**PART II**

**Figure 2b.** Summary of the methodological approach (Part II: Socio-economic risk analysis)

## Indicators of exposure and vulnerability

To understand the impact risks to cities from flooding and drought, we first state the indicators used to factor in exposure and vulnerability. For a full definition of how we calculate risk, please see the **Definitions.**

This analysis focuses on the global scale, requiring detail to be weighed against the possibility of gaining a larger, consistent overview of flood and drought risk for the 97 C40 cities. Our approach makes use of state-of-the-art global-scale models, resulting in first-cut cost estimates. These outline the potential impact a drought or flood could have on each city, so can be used to raise awareness. **It should be noted that our estimates do not include all potential flood and drought impacts. For example, we only examine direct impacts and do not look at the indirect impacts or 'chain effects' that these hazards can cause.** Such chain effects are often event and location specific, and methods to assess them are still difficult to implement in global disaster risk models, as they need highly accurate input data.[39] Moreover, we do not examine the potential impacts of floods and drought across all potentially impacted sectors, as we would have to take into account all chain effects to do so.


## Flooding

Flood exposure centres on three metrics: (1) population, (2) GDP and (3) urban land use. We estimate the first two using global datasets for population and GDP, each with a spatial resolution of 30” x 30”.[40] These datasets include forecasts of the current situation and future socio-economic scenarios (SSPs) in the form of total population estimates per grid cell and total GDP per grid cell in 2005 US dollar terms.[41] We chose this price unit because it is commonly used in disaster risk studies,[42] thus facilitates cross-study comparability. We modelled the urban land-use indictor using the 2UP model developed by the Netherlands Environmental Assessment Agency (PBL).[43] This model is essentially an urban/non-urban land-use dataset that estimates the percentage of build-up in urban areas. Every urban land-use cell in 2UP has a fixed mix of three urban categories - residential, commercial and industrial - and each class is assigned its own maximum potential damage level. The spatial resolution of the data is 30” x 30” and the data are available for the current situation and future scenarios using SSPs.

We express flood vulnerability using depth-damage curves, which depict the relationship between a certain depth of inundation (water level) and the expected costs for a certain type of building and/or location. In essence, a flood with a low inundation depth causes less damage than a flood with high inundation depth.[44] This is predominantly associated with the urban land-use exposure metric.

**Infrastructure exposure**

We also use two other metrics to denote the global (change in) vulnerability under different climate scenarios: **(1) the number of power stations affected and (2) the number of hospitals and healthcare facilities affected.** These are both defined as the total number of power stations/hospitals located in inundated grid cells. Taking global datasets for hospitals[45] and power stations and overlaying them with our inundation maps, we selected the hospitals and power stations located in a given city. We then overlaid the hospitals and power stations with the flood hazard maps. We then counted the number of hospitals and power stations[46] in the inundated zone (inundated zone = all pixels that had a flood volume > 0) and noted their ID numbers/names. We did this for every flood hazard map, so for every combination of climate model (GCM), climate scenario (historical, RCP 4.5 and RCP 8.5) and return period.

We did not consider local flood adaptation measures (such as elevated building sites or flood walls), so not all exposed stations or hospitals are likely to be affected. These buildings are units of critical infrastructure, however, and flooding can have relatively far-reaching effects on them and the cities they serve. Therefore, these metrics are intended to show the potential global number of critical infrastructure units within the exposed area as a measure of the overall vulnerability of the cities.

## Drought

Conventional exposure metrics used in flooding do not fit with the current approach to calculating drought risk in cities. The elements exposed to drought are inherently included in the hazard analysis for this study. For agricultural drought, the exposed elements are the agricultural areas in the water province(s) surrounding a city, while for hydrological drought, the exposed elements are the surface water-source locations and city populations. In this sense it is not possible to state the number of people in a city who are exposed to both hydrological and agricultural drought, as the city as a whole experiences drought, so the population within the city does as well.

Drought vulnerability is not inherent in the hazard analysis, but included qualitatively after the socio-economic impact estimates in the *Water-safe narratives*. Vulnerability is represented by several metrics, depending on data availability and the link between the drought hazard and its impact on the exposed elements. These indicators are listed in Table 4.

## Step 3:
# Calculating socio-economic impacts

### Flooding

The ingredients of the hazard, exposure and vulnerability metrics described in the previous sections could now be integrated into a socio-economic impact risk) estimate for each of the C40 cities. We overlaid the flood hazard maps for the different combinations of GCM, RCP and return period with population and GDP maps for the different SSPs. This resulted in a set of maps encompassing th e affected population and GDP per grid cell for each unique combination of GCM, RCP, SSP and return period. We also overlaid the urban land-use map for the different SSPs with the flood hazard maps. The percentage of urban built-up was then subdivided into commercial, residential and industrial build-up areas and linked to their corresponding depth-damage curves. These damages were summed to get total damage per grid cell. This gave us urban damage per GCM, RCP, SSP and return period combination. We then added up the impacts for each combination of GCM, RCP, SSP, return period and impact type for each individual city. Note that GCMs are relevant to riverine flooding but not coastal flooding.

### Drought

We estimated drought costs by calculating the cost of freshwater production/saving as a proxy. The need to use a proxy stemmed from the absence of an applicable method for calculating drought costs in urban regions on a global scale. Drought can have myriad (in)direct impacts that are hard to quantify, as described previously. The rationale for using the cost of freshwater production/saving was that this would quantify the cost of solving a drought of volume X, by producing X amount of water to maintain business as usual and, thus, prevent any other impacts from occurring. Although these costs are based on adaptation measures, we do not regard them as the true costs of adaptation. The measures chosen are all primarily mitigating solutions: they do not prevent drought, nor are they long-term, sustainable solutions.

Freshwater production cost/savings are based on three adaptation measures for which global unit cost estimates are available from the water scarcity literature.[47] These measures are: (1) the increase in reservoir storage capacity, (2) the reuse of urban residential/industrial water and (3) the increase in desalination (Table 4).

Increased reservoir capacity costs are estimated based on Ward et al. (2010a). They vary from water province to province and are based on the relationship between mean basin slope and the unit cost per $m^3$ for 11 different reservoir sizes. Each water province used in this study was assigned a value from a water province in Ward et al. (2010a), based on the largest overlap, because the shapes occasionally differed from the more recent version of the report used here Straatsma et al. (2020).

There are two elements to the costs of desalination: a constant value of US$ 1/$m^3$ conversion cost and a variable price for water transport between the city and the nearest coastline.[49] Coastlines are obtained from Natural Earth and come from the coastline dataset V4.1.0.[50] The transportation costs are divided into a horizontal and a vertical component, which carry a unit cost of US$ 0.05/$m^3$ per 100 km and US$ 0.05/$m^3$ per 0.1 km, respectively (see Table 4). Horizontal transportation distances are determined

| Adaptation measure | Unit cost (US$ 2005/$m_3$) | Source |
|---|---|---|
| Increase reservoir storage capacity | Variable between water provinces | Ward et al. (2010a) |
| Reuse urban residential/industrial water | Variable between water provinces | Straatsma et al. (2020) |
| Increase desalination | 1 (constant component) + 0.05 per 100 km horizontal or 0.1 km vertical transport (variable | Straatsma et al. (2020); Zhou & Tol (2005) |

**Table 4.** Global average unit cost of freshwater production as found in the cited literature



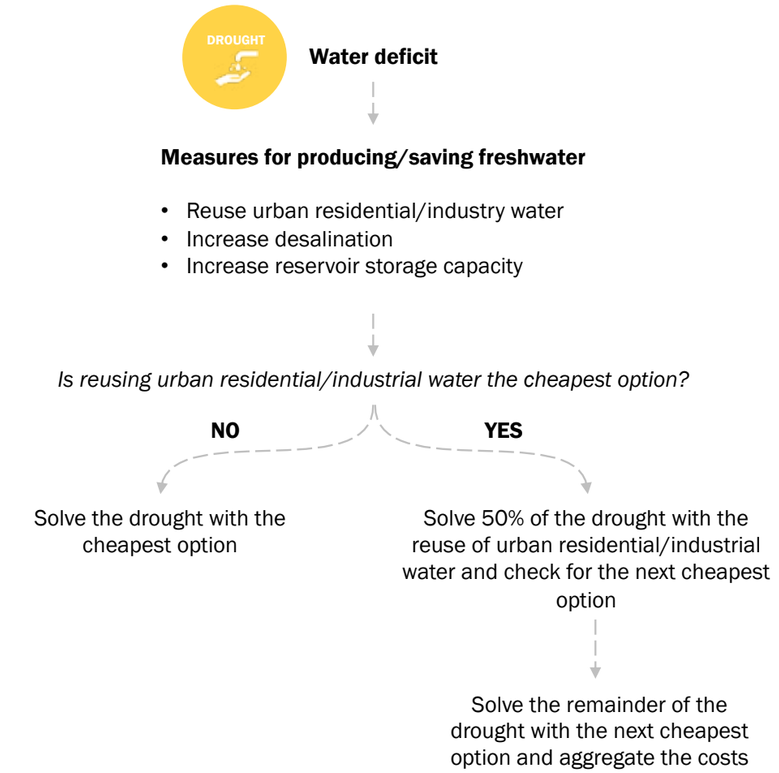


**Figure 7.** Process for calculating the cost of hydrological drought

by measuring the shortest linear distance between a city's boundaries (as derived from GHS-SMOD) and the nearest coastline, using QGIS 3.10.11. The vertical transportation distance is the sum of all absolute height differences between consecutive pixels from the Shuttle Radar Topography Mission Digital Terrain Model (SRTM DTM)[51] V4.1 that intersect with the horizontal transport line. The SRTM DTM has a resolution of 3 arcseconds (3). Lastly, we have taken the costs of reusing urban residential or industrial water as a global constant of US$ 0.3 per $m^3$.[52]

For each city-RCP combination, we calculated the minimum and maximum drought costs. We had to take a scenario approach here, as the literature contained no exclusions to a suitable or achievable mix of the three adaptation options. This probably varies by city, local situation and characteristics (for example, how much of the renewable surface water has already been consumed). Hence, for each city-RCP scenario, we calculated both the cost based on the cheapest solution and the cost based on the priciest solution to give a range for the potential cost of freshwater production. We also capped the reuse of urban residential/industrial water at 50% of total drought volume, so it would only cover 50% of the total freshwater production needed to maintain business as usual. No global average or spatially varying number for this cap could be found in the literature, with examples ranging from 5% to 100% percent,[53] depending on which residential/industrial water use was reused.[54] We thus chose a mid-way solution of 50%. Estimates of desalination and reservoir capacity most often seemed capable of meeting the drought volumes in this study, so were not capped.[55] See Figures 5a and 5b for a flow chart summarising these steps.

**Socio-economic analysis:**
**Hydrological drought assumptions**

Even though drought volumes might be overestimated, drought costs are likely to be underestimated. We assume that the cost of water production/saving is a suitable proxy for actual drought cost and that the true drought costs are somewhere in between the minimum and maximum costs estimated here. Although this gives a reasonable estimate of the order of magnitude, the true costs are probably higher than the maximum costs estimated here due to chain effects within or outside the city's economy. Actual drought costs - both direct and indirect - remain difficult to estimate, as the hazard is intangible. This makes it hard to discriminate between pure drought-related impacts and impacts that happen during but independently of the drought.

Each water-production/-saving measure is assumed to be capable of fully solving each drought volume as estimated here, except for the reuse of urban residential/industrial water, which is capped at 50% of the total drought volume. Actual limits may differ from those assumed in this assessment due to high costs, physical production limitations or insufficient space for desalination facilities or dams, for instance. No further information on those limits was found and research on a local scale is needed to track down the corresponding numbers for this. Furthermore, desalination is assumed to be applicable anywhere, but could be relatively expensive for inland cities that have no saltwater bodies nearby, so need to transport water over large distances.

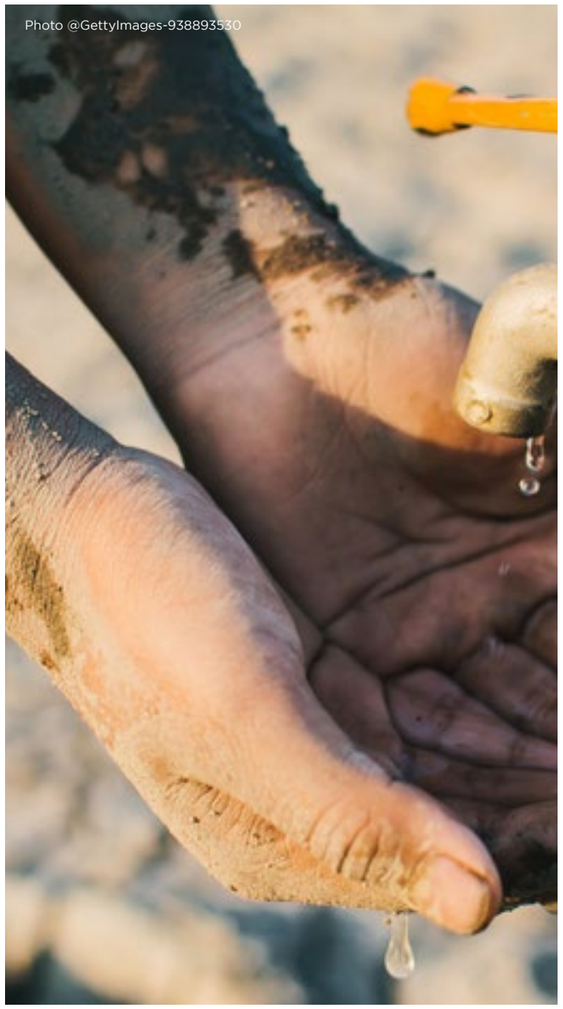


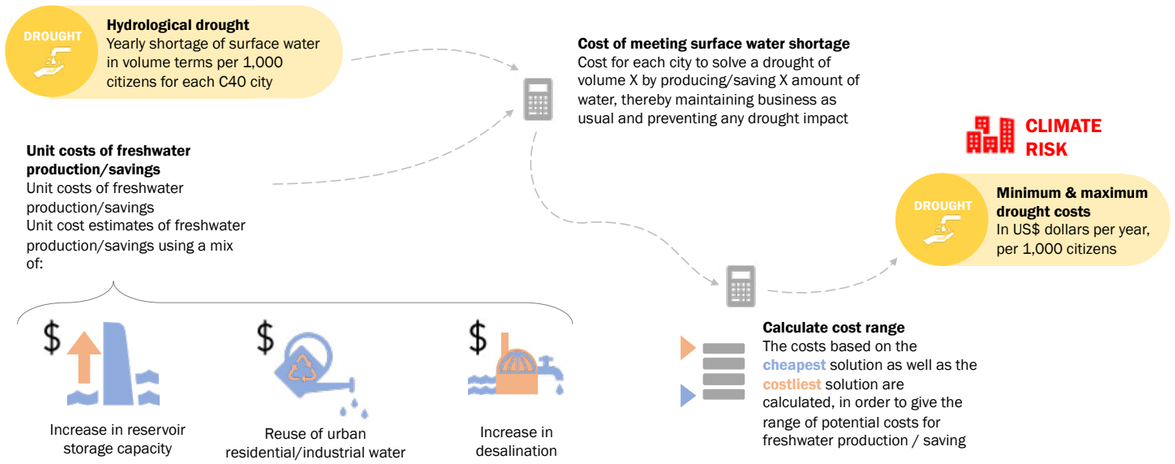


**Figure 8:** A visual summary of the methodology behind our assessment of socio-economic risk (cost to replace water deficit) from hydrological drought



## Step 4:
## Estimating probabilistic risk

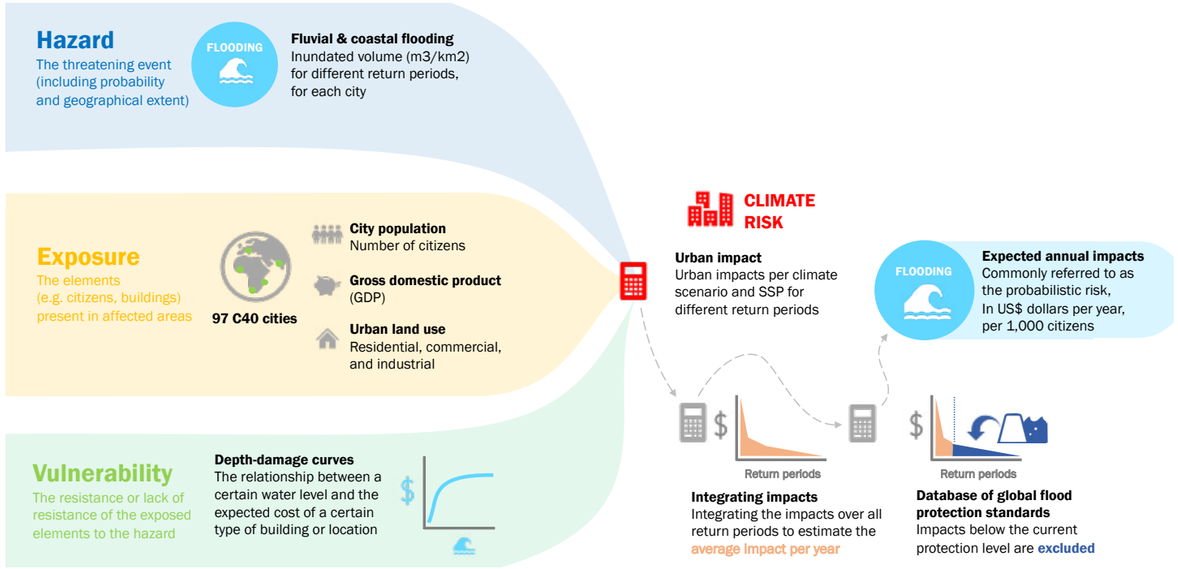


**Figure 9.** Visual summary of the methodology behind our assessment of flood risk

After calculating the socio-economic impacts for the various return periods, we estimated the expected annual impacts (EAIs), commonly referred to as the probabilistic risk. This step was only required for riverine and coastal flooding, as our hydrological drought calculations did not use return periods and already included an estimated annual damage value from the previous step.

We calculated the EAI by integrating the impacts (the damages, exposed GDP or exposed population) over all of the different return periods, which effectively gave an estimate of the average impact per year (expected annual damage, expected number of people affected per year, expected effect on GDP per year). In the EAI, we included the impacts for each city for each possible GCM combination (riverine flooding only), RCP, SSP and impact type. In reality, there were many years with no impact and only one or a few years with a very high impact. The EAI indicators thus denote the average of all of these years.

**Standardising EAIs**

For each city, the EAI for riverine and coastal flooding and for hydrological drought is standardised per 1,000 inhabitants. The reason for this is that total impacts are likely to be higher for larger cities, as these have greater populations, more buildings and a larger GDP (exposed elements) to be impacted. Part of this bias is taken away by standardising the EAIs for population. In other words, the standardised values denote the impact regardless of size.

It is crucial to account for the fact that many regions of the world (mainly cities) are protected against flooding, for example, by dykes or levees. If these are ignored, as they are in most large-scale flood risk estimates, the risk will be grossly overestimated. To address this issue, IVM developed a database of global flood protection standards (FLOPROS),[56] which we used in this study to exclude impacts for flood events below the current design standard for dykes and levees. It should be noted that FLOPROS includes three layers of protection standard based on three source categories: (1) the design layer, which holds information on an empirical basis and represents currently installed protection; (2) the policy layer, which fills gaps in the design layer where possible and holds information on policy regulations; (3) the model layer, which plugs any remaining gaps by modelling the protection standards in areas where no empirical or policy information is available.[57] Hence, FLOPROS includes protection standards that are already in place (design layer) and those that are desirable (policy and model layers). The latter may also be in place, but this could not be confirmed or denied from the data. Therefore, if there is a protection standard in place that guards the city against a flood event with a return period of 10 years, which equates to a 10% exceedance probability per year, all flood events with a return period of 10 years or less should not cause any damage to the city.


# 6. Definitions

## Climate risk


**Figure 10.** A visual definition of climate risk

The Intergovernmental Panel on Climate Change's (IPCC) Fifth Assessment Report (AR5) offers a conceptual framework for the assessment of risks associated with climate change.[58] Climate risk is caused by harmful climate events that have negative impacts on cities worldwide. The consequences are the result of the interplay between the hazards and what is referred to as components of exposure and vulnerability. We follow the definitions of the United Nations Office for Disaster Risk Reduction (UNDRR) in this project. The following definitions of hazard, exposure, and vulnerability are from the UNDRR glossary,[59] along with a short addendum or explanation on each.



**Hazard**
A process, phenomenon or human activity that may cause loss of life, injury or other health impacts, property damage, social and economic disruption or environmental degradation.[60] It is a threatening event, including in terms of its probability and geographical extent. Note the word 'may', which implies that an event does not always cause (negative) impacts, as these depend on the exposure and vulnerability components.

**Climate risk**
The potential loss of life, injury or destroyed or damaged assets that could occur to a system, society or a community in a specific period of time, determined probabilistically as a function of (1) a climate-related hazard, (2) exposure, (3) vulnerability.[63] Therefore, in facing a climate hazard, people, assets and natural resources may be exposed and vulnerable in different ways, depending, among other things, on their location and capacity to cope and adapt. The interplay of a hazard, the exposed elements and their vulnerability determines climate risk.

**General circulation models (GCMs):** A model that predicts the climatic state of the earth based on a set of boundary conditions, namely solar radiation and GHG concentration.

**Shared socio-economic pathways (SSP):** SSPs represent a set of scenarios - or plausible future worlds - that underpin climate change research and permit the integrated analysis of future climate impacts, vulnerabilities, adaptation and mitigation, including possible pathways for global society, economics and demographics. They can be categorised by the degree to which the different scenarios represent challenges to mitigation (reducing the sources or enhancing the sinks of GHGs) and societal adaptation to climate change.

**Representative concentrated pathway:** RCPs are trajectories of greenhouse gas concentrations resulting from human activity corresponding to a specific level of radiative forcing in 2100.

**Return period:** For example, if a flood of volume X happens statistically once every 100 years, the return period of that flood is said to be 100 years.

**Rootzone moisture:** The volume of moisture in the top 1 metre of soil in a given area.

**Exposure**
The situation of people, infrastructure, housing, production capacities and other tangible human assets located in hazard-prone areas.[61] These are all the elements present in affected areas, such as citizens, flora and fauna, buildings and (critical) infrastructure.

**Vulnerability**
The conditions determined by physical, social, economic and environmental factors or processes which increase the susceptibility of an individual, a community, assets or systems to the impacts of hazards.[62] This is the (lack of) resistance of the exposed elements to the hazard.

**Water province:** A water province is a spatial unit of watersheds that belongs to exactly one country and one watershed area. If a water province is shared by multiple cities, we assume that the total water shortage is split equally among these cities. Where a city intersects with more than one water province, we add up the water deficits of all corresponding water provinces. Thus, each city is assigned their share of water shortages from adjacent water provinces.

# Annex 1.
# Possibilities and limitations of global-scale models

## Flooding

**Riverine flooding**
Global riverine flood risk assessments generally include a full suite of hazard, exposure and vulnerability components.[64] They have sporadically incorporated hazard and exposure dynamically. Dynamic vulnerability has only been included once, however.[65] In all other cases, static hazard/exposure/vulnerability data were used. The spatial resolution of global-scale analyses in the most recent studies has varied from 30 arcseconds (“) to 2.5 arcminutes (‘).[66] Hazard has often been expressed as the depth and extent of inundation, population exposure, GDP or land use and vulnerability by depth-damage function.[67] To arrive at estimated flood areas and flood maps, most global models do not use a full hydrodynamic modelling scheme, as this requires high-resolution topographical features that are not yet available and have a high computational cost.[68] Rather, like us, they compute discharge and use a volume-spreading approach to determine flooded areas.

**Coastal flooding**
Global coastal flood risk assessments are similar to riverine ones. They also consider all risk components, sporadically incorporating dynamic hazard and exposure. However, dynamic vulnerability has not yet been included. Spatial resolutions deviate slightly from riverine flood risk assessments too, varying between coastline segments and gridded fields of 30 arcseconds (30”). Still, the risk components are explained using the same parameters as for riverine flooding. Although sea levels are calculated using a fully hydrodynamic model, the flood levels on land are not - a challenge similar to that discussed for riverine flooding.[69]

**Stormwater flooding**
Assessing stormwater flooding on a global scale is difficult, as it is highly dependent on local factors. To the best of our knowledge, the scientific literature does not contain any examples of global-scale stormwater flood risk assessments. It is most commonly assessed using flood models for a small area (such as city or even part of a city) that generate data on the depth and velocity of surface water associated with rainfall events of varying intensity. Guerreiro et al. (2017) have developed a continental-scale modelling approach to assess the stormwater flood hazard for 571 cities in Europe. The paper outlines some of the key challenges of such a continental approach, which would be amplified in the case of global-scale application. These include difficulties in obtaining the required hourly rainfall records, the low resolution of continental to global digital elevation models (DEMs) compared with those typically used for stormwater flood models, and a lack of data on local sewer systems, building shapes and infiltration of local green spaces. Opportunities to collect such data lie in high-resolution remote sensing and data science,[70] but also in local crowdsourced methods, such as community mapping,[71] which is a promising avenue, particularly in strongly growing urban centres in developing countries. Guerreiro et al. (2017) demonstrate that current modelling capabilities and the requisite computing power make large-scale stormwater flood hazard assessment a possibility, provided these data challenges can be overcome. However, to include stormwater flooding in this research, we use the change in extreme rainfall as a proxy (see section 5.4.2).

## Drought

Due to their complex and diverse character, it is often difficult to find a comprehensive set of indicators for drought risk. This has led to a variety of approaches and datasets in global drought risk assessments. According to Ward et al. (2020), these assessments generally include indicators for the hazard itself and the corresponding exposure. Vulnerability has sporadically been included, but not yet dynamically. The spatial resolution of global drought risk assessments has been 0.2-0.5 degrees. As summarised by Ward et al. (2020), drought hazards have been expressed through a multitude of different indices, such as the Standardized Precipitation Index (SPI), Standardized Precipitation and Evapotranspiration Index (SPEI), Standardized Runoff Index (SRI), Palmer Drought Severity Index (PDSI) and the Weighted Anomaly of Standardized Precipitation (WASP). Exposure has been expressed as the effect on the population, GDP, road density, agricultural area and/or crop yields. Vulnerability is represented by the proportion of area irrigated per country or by proxies of social, economic and infrastructural vulnerability (for example, GDP per capita, government effectiveness or percentage of irrigated agricultural land).[72] Lastly, the risk is expressed using indicators such as maize yield losses or agricultural area or population affected.[73]



# Annex 2.
# Qualitative hydrological drought methodology

The above methodology resulted in several C40 cities[74] lacking a hydrological analysis for one of the following reasons:

- According to the CWM database, the city only had one groundwater source.
- The city was present in the database, but had no withdrawal point to link it to discharge.
- The city was not in the CWM database.
- The city was in the CWM database, but there was no information on its surface water sources.

Consequently, a methodology had to be developed to qualitatively assess the impacts of hydrological drought on these cities. The cities for which data were missing are included in Table 2.

To assess the relative impacts and benefits associated with the availability of urban water resources and their risk of hydrological drought, we used a multi-criteria analysis, comparing five indicators and evaluating different combinations.

Five indicators were used: (1) water supply stress (WSS), (2) water-source type distribution (WST), (3) number of sources (S), (4) CDP drought intensity (CDP) and (5) recent drought activity (DA) (see details in Table 7). By assigning weights[75] to each indicator, it was possible to assess the drought impact in terms of these indicators. With each indicator carrying a maximum score of three, the total maximum score a city could have was 15.[76]

We conducted two multi-criteria analyses using these indicators. The first included all the indicators with the exception of cities that did not have any CDP reporting.

**Sample calculations**
**City with CDP reporting:** WSS+WST+S+CDP+DA/15
**City without CDP reporting:** WSS+WST+S+DA/12

The second analysis excluded any indicator for which the original status was not available. This included water supply stress and CDP for which cities either did not have water supply stress data or they had not reported to CDP.

**Sample calculations**
**City with CDP reporting:** WSS+WST+S+CDP+DA/15
**City without CDP reporting:** WSS+WST+S+DA/12
**City without water supply stress data:** CDP+WST+S+DA/12
**City without water supply stress data or CDP reporting:** WST+S+DA/9

Both analyses had a minimum indicative percentage of 33% and a maximum percentage of 100%, due to the weighting of each indicator. For the final score, an average of the results of the two analyses was used for each city.

To verify this methodology, it was applied to a regionally representative group of cities for which IVM had data.[77] As the normalised percentages could not be quantitatively compared with the water-source volume difference for the 10-year return period, the ordinal ranking of the cities, from lowest risk to highest risk of drought, was used (see Table 5 ). Of the cities for which we had data, only three were not within 1 ordinal ranking when comparing the C40 and IVM rankings, namely, New York, Delhi and Santiago.

| Rank | C40 ranking | Indicative percentage | Population | IVM ranking |
|---|---|---|---|---|
| 1 | **Stockholm** | 67% | 1,485,000 | **Stockholm** |
| 2 | **Accra** | 75% | 3,013,000 | **Accra** |
| 3 | **Nairobi** | 75% | 3,958,000 | **Nairobi** |
| 4 | **New York** | 75% | 8,468,000 | **Jakarta** |
| 5 | **Jakarta** | 75% | 10,470,000 | **Beijing** |
| 6 | **Beijing** | 75% | 18,079,000 | **Santiago** |
| 7 | **Delhi** | 75% | 25,629,000 | **Sydney** |
| 8 | **Sydney** | 77% | 4,844,000 | **London** |
| 9 | **London** | 77% | 9,348,000 | **Rio de Janeiro** |
| 10 | **Rio de Janeiro** | 80% | 12,380,000 | **New York City** |
| 11 | **Santiago** | 87% | 6,355,000 | **Delhi** |
| 12 | **Los Angeles** | 87% | 14,081,000 | **Los Angeles** |

**Table 5.** Ordinal hydrological drought ranking of cities

The methodology was applied to all C40 cities for which data were missing. The results can be seen in Table 2. Using the indicative percentages for risk, we created a risk profile for all of the cities in the analysis based on the Likert scale (see Table 6). Cities were grouped into their corresponding categories based on this scale.



| Rank | City[i] | Indicative percentage | Rank | City | Indicative percentage |
|---|---|---|---|---|---|
| 1 | Zhenjiang | 53% | 21 | Beijing | 75% |
| 2 | Hangzhou | 58% | 22 | Curitiba | 75% |
| 3 | Shenzhen | 58% | 23 | Delhi | 75% |
| 4 | Berlin | 60% | 24 | Jakarta | 75% |
| 5 | Fuzhou | 60% | 25 | Nairobi | 75% |
| 6 | Rome | 60% | 26 | New York | 75% |
| 7 | Madrid | 60% | 27 | Shanghai | 75% |
| 8 | Dubai | 63% | 28 | Washington, D.C. | 75% |
| 9 | Kuala Lumpur | 63% | 29 | Johannesburg | 77% |
| 10 | Milan | 63% | 30 | London | 77% |
| 11 | Singapore | 63% | 31 | Sydney | 77% |
| 12 | Medellín | 67% | 32 | Cape Town | 80% |
| 13 | Stockholm | 67% | 33 | Melbourne | 80% |
| 14 | Abidjan | 71% | 34 | Rio | 80% |
| 15 | Quezon City | 71% | 35 | Copenhagen | 82% |
| 16 | Ekurhuleni | 72% | 36 | Hanoi | 82% |
| 17 | Jaipur | 72% | 37 | Durban (eThekwini) | 83% |
| 18 | Miami | 72% | 38 | Seoul | 83% |
| 19 | Lima | 75% | 39 | Los Angeles | 87% |
| 20 | Accra | 75% | 40 | Santiago | 87% |
| | | | 41 | New Orleans | 92% |

**Table 6.** Cities' indicative risk table based on the Likert Scale

| Indicator name | Description | Rating description | | | Source |
|---|---|---|---|---|---|
| | | 1 | 2 | 3 | |
| **Water supply stress** | Annual stress is defined as the ratio of water withdrawn from a watershed to water available. By convention, a value above 0.4 is defined as stressed. The Urban Water Blueprint only evaluates surface water sources | N/A (missing information or primary sources are not surface water) | No (a value below or equal to 0.4) | Yes (a value above 0.4) | McDonald and Shemie (2014) |
| **Water-source type distribution** | The water-source typology categorised to include groundwater, surface water and desalination/other sources | Source mix, with no singular source type accounting for more than 50% | More than 50% of water sources are groundwater | More than 50% of water sources are surface water | |
| **Number of sources** | The total number of water sources from which the city abstracts its water | City has more than four water sources | City has fewer than four water sources | City has a single water source | |
| **CDP drought intensity** | A combined metric of probability and magnitude[ii] of drought reported to the CDP by cities | Cities with a low drought intensity | Cities with a medium drought intensity | Cities with a high drought intensity | CDP reporting by cities |
| **Recent drought activity** | Drought[v] reported within a given city within the last 15 years | No drought reported | Single one-year drought reported | Multiple or multi-year drought reported | Multiple sources |

**Table 7.** Criteria used for the evaluation

# Annex 3.
# Data sources

| Name | Description | Source |
|---|---|---|
| *Inter-Sectoral Impact Model Intercomparison Project* | Bias-corrected global gridded climate data. | https://www.isimip.org/ |
| *(ISIMIP Fast Track)* | | |
| *WATCH WFDEI* | Global gridded climate data for the 1901-2012 period, based on reanalysis datasets. | https://www.isimip.org/ |
| *City Water Map (CWM) Database* | Database that holds information on water extraction points and, wherever possible, withdrawal volumes for 534 cities globally, based on web searches. | https://knb.ecoinformatics.org/view/doi%3A10.5063%2FF1J67DWR |
| *Spatial Production Allocation Mode (MapSPAM)* | Gridded map of the distribution of physical agricultural areas of 42 common crop types, based on a variety of input data. | https://www.mapspam.info/ |
| *2UP* | Global simulation of future urban growth, population distributions, and sub-national GDP developments, all based on SSPs. | https://www.pbl.nl/sites/default/files/downloads/pbl-2018-Towards-an-urban-preview_3255.pdf |
| *Global Human Settlement - Settlement Model Grid (GHS-SMOD)* | Global shapefile of city borders based on (1) population totals, (2) population densities and (3) build-up densities. | https://ghsl.jrc.ec.europa.eu/ghs_smod2019.php |
| *Water provinces* | Shapefile of intersections between administrative country borders and watershed borders. Each water province thus lies solely in one country and one watershed. | https://www.sciencedirect.com/science/article/pii/S1364815218311447?casa_token=CgeXCjZv3NgAAAAA:uw6g7pw4MGjn9-vr42bBMqK9EZQw4Zeur3i_lYdScDFvCIfgdaZISrytE2hmJUJ5pZjfExILDJE |
| *Natural Earth 10m coastlines* | Global vector dataset of coastlines based on World Data Bank 2 and NASA Mosaic of Antarctica. | https://www.naturalearthdata.com/downloads/10m-physical-vectors/10m-coastline/ |
| *Shuttle Radar Topography Mission Digital Terrain Model 90m V4.1* | Relatively high-resolution global map of elevation based on satellite imaging. | https://cgiarcsi.community/data/srtm-90m-digital-elevation-database-v4-1/ |
| *Depth-damage curves* | These curves depict the relationship between a certain inundation depth (water level) and the expected costs for a certain type of building and/or for a certain location. These ones are construction cost surveys from multinational construction companies and are specified for each individual country. | https://publications.jrc.ec.europa.eu/repository/handle/JRC105688 |
| *FLOod PROtection Standards (FLOPROS) Database* | FLOPROS provides information on flood protection standards on a sub-national level (in this research). It is based on (1) empirical information where available, (2) policy regulations wherever available and where no empirical information is available, (3) modelling results for all other places. | https://research.vu.nl/en/publications/flopros-an-evolving-global-database-of-flood-protection-standards |
| Multi-Error-Removed Improved-Terrain (MERIT) Digital Elevation Model | | http://hydro.iis.u-tokyo.ac.jp/~yamadai/MERIT_DEM/ |
| PCR-GLOBWB | A global hydrological model developed by Van Beek and Bierkens (2009) and Van Beek et al (2011). It is forced with gridded climate data. For the current period (1960-99), the model is forced with EU-WATCH forcing data (Weedon et al., 2011). For the future, it is forced using bias-corrected | https://github.com/UU-Hydro/PCR-GLOBWB_model |
| *(Geophysical Fluid Dynamics Laboratory – Earth Systems Model)* *GFDL-ESM2M* | One of the GCMs used to capture the complex dynamics on Earth that make up the climate. Each GCM tries other sets of assumptions and methods to perform their calculations. As there is no 'best' model, scientists usually aim to use a couple of GCMs and take an average or median value from them to get a robust outcome of the future climate. | https://www.gfdl.noaa.gov/earth-system-model/ |
| *HadGEM2-ES* | One of the GCMs used to capture the complex dynamics on Earth that make up the climate. Each GCM tries other sets of assumptions and methods to perform their calculations. As there is no 'best' model, scientists usually aim to use a couple of GCMs and take an average or median value from them to get a robust outcome of the future climate. | https://www.metoffice.gov.uk/research/approach/modelling-systems/unified-model/climate-models/hadgem2 |
| *IPSL-CM5A-LR* | One of the GCMs used to capture the complex dynamics on Earth that make up the climate. Each GCM tries other sets of assumptions and methods to perform their calculations. As there is no 'best' model, scientists usually aim to use a couple of GCMs and take an average or median value from them to get a robust outcome of the future climate. | https://cmc.ipsl.fr/international-projects/cmip5/ |
| *MIROC-ESM-CHEM* | One of the GCMs used to capture the complex dynamics on Earth that make up the climate. Each GCM tries other sets of assumptions and methods to perform their calculations. As there is no 'best' model, scientists usually aim to use a couple of GCMs and take an average or median value from them to get a robust outcome of the future climate. | https://catalogue.ceda.ac.uk/uuid/d90ca0077e3344c7840ca56e49f89ee7 |
| *NorESM1-M* | One of the GCMs used to capture the complex dynamics on Earth that make up the climate. Each GCM tries other sets of assumptions and methods to perform their calculations. As there is no 'best' model, scientists usually aim to use a couple of GCMs and take an average or median value from them to get a robust outcome of the future climate. | https://gmd.copernicus.org/articles/6/687/2013/gmd-6-687-2013.html |

# Annex 4.
# Resolution tables

Throughout our analysis we have had to used varying models with differing levels of resolution. We summarise the resolution of all datasets below.

| Climate hazard and socioeconomic analysis | Indicator | Resolution |
|---|---|---|
| Riverine flooding | Flood volume per pixel | 30” x 30” (around 1 km x 1 km at the equator) |
| Coastal flooding | Flood volume per pixel | The model resolution is 2.5 km from the coast (1.25 km in Europe). |
| Stormwater flooding | Change in the frequency of a one-in-10 year precipitation event | 0.5o x 0.5o |
| Population and GDP | | 30″ x 30″ |
| Urban land use indicator from the 2UP model. The model has a fixed mix of three urban categories – residential, commercial and industrial – and each class is assigned its own maximum potential damage. | | 2UP resolution = 30”x 30” |

# References


Agnew, C.T. (2000). Using the SPI to Identify Drought. Drought Network News, 12(1), 6–12.

Anderson, J. (2003). The environmental benefits of water recycling and reuse. Water Science and Technology: Water Supply, 3(4): 1–10. https://doi.org/10.2166/ws.2003.0041

Bauer, S., Linke, H.J. and Wagner, M. (2020). Combining industrial and urban water-reuse concepts for increasing the water resources in water-scarce regions. Water Environment Research, 92(7): 1027–1041. https://doi.org/10.1002/wer.1298

Below, R., Grover-Kopec, E. and Dilley, M. (2007). Documenting Drought-Related Disasters. The Journal of Environment & Development, 16(3): 328–344.

Breyer, B., Zipper, S.C. and Qiu, J. (2018). Sociohydrological Impacts of Water Conservation Under Anthropogenic Drought in Austin, TX (USA). Water Resources Research, 54(4): 3062–3080. https://doi.org/10.1002/2017WR021155

Burian, J., Pastzo, V. and Langrova, B. (2014). Possibilities of the Definition of City Boundaries in GIS The Case Study of a Medium-Sized City. Cartography and GIS, 3: 777 784.

Buurman, J., Mens, M.J.P. and Dahm, R.J. (2016). Strategies for urban drought risk management: a comparison of 10 large cities. International Journal of Water Resources Development, 33(1): 31–50. https://doi.org/10.1080/07900627.2016.1138398

Carrão, H., Naumann, G. and Barbosa, P. (2016). Mapping global patterns of drought risk: An empirical framework based on sub-national estimates of hazard, exposure and vulnerability. Global Environmental Change, 39: 108–124. https://doi.org/10.1016/j.gloenvcha.2016.04.012

Carrera, L., Standardi, G., Bosello, F. and Mysiak, J. (2015). Assessing direct and indirect economic impacts of a flood event through the integration of spatial and computable general equilibrium modelling. Environmental Modelling and Software, 63: 109–122. https://doi.org/10.1016/j.envsoft.2014.09.016

Chbab, E.H. (1995). How extreme were the 1995 flood waves on the rivers Rhine and Meuse? Physics and Chemistry of the Earth, 20(5–6): 455–458. https://doi.org/10.1016/S0079-1946(96)00005-5

Department of Water and Sanitation (2019). 2018/19 Annual Report Vote 36. Pretoria, South Africa: National Treasury. http://www.treasury.gov.za/documents/national%20budget/2019/ene/Vote%2036%20Water%20and%20Sanitation.pdf

Dracup, J.A., Lee, K.S. and Paulson, E.G. (1980). On the definition of droughts. Water Resources Research, 16(2): 297–302. https://doi.org/10.1029/WR016i002p00297

Dullaart, J.C.M., Muis,S., Bloemendaal, N. and Aerts, J.C.J.H. (2020). Advancing global storm surge modelling using the new ERA5 climate reanalysis. Climate Dynamics, 54: 1007–1021. https://doi.org/10.1007/s00382-019-05044-0

Dutra, E., Viterbo, P. and Miranda, P.M.A. (2008). ERA-40 reanalysis hydrological applications in the characterization of regional drought. Geophysical Research Letters, 35(19): 2–6. https://doi.org/10.1029/2008GL035381

Florczyk, A.J., Corbane, C., Ehrlich, D., Freire, S., Kemper, T., Maffenini, L. et al. (2019). GHSL Data Package 2019 Technical report by the Joint Research Centre (JRC), European Union. Brussels: Joint Research Centre. https://doi.org/10.2760/0726

Flörke, M., Schneider, C. and McDonald, R.I. (2018). Water competition between cities and agriculture driven by climate change and urban growth. Nature Sustainability, 1(1): 51–58. https://doi.org/10.1038/s41893-017-0006-8

Global Commission on Adaptation (GCA) (2019). Adapt now: a global call for leadership on climate resilience. Rotterdam, the Netherlands. https://gca.org/reports/adapt-now-a-global-call-for-leadership-on-climate-resilience/

Guerreiro, S. B., Glenis, V., Dawson, R.J. and Kilsby, C. (2017). Stormwater flooding in European cities-A continental approach to urban flood modelling. Water (Switzerland), 9(4). https://doi.org/10.3390/w9040296

Güneralp, B., Güneralp, I. and Liu, Y. (2015). Changing global patterns of urban exposure to flood and drought hazards. Global Environmental Change, 31: 217–225. https://doi.org/10.1016/j.gloenvcha.2015.01.002

Hagenlocher, M., Meza, I., Anderson, C.C., Min, A., Renaud, F.G., Walz, Y., Siebert, S. and Sebesvari, Z. (2019). Drought vulnerability and risk assessments: State of the art, persistent gaps, and research agenda. Environmental Research Letters, 14(8). https://doi.org/10.1088/1748-9326/ab225d

Hallegatte, S., Vogt-Schilb, A., Bangalore, M. and Rozenberg, J. (2017). Unbreakable. Building the Resilience of the Poor in the Face of Natural Disasters. Washington, DC: World Bank. https://openknowledge.worldbank.org/handle/10986/25335

Hanasaki, N., Yoshikawa, S., Kakinuma, K. and Kanae, S. (2016). A seawater desalination scheme for global hydrological models. Hydrology and Earth System Sciences, 20(10): 4143–4157. https://doi.org/10.5194/hess-20-4143-2016

Hao, Z. and Singh, V.P. (2015). Drought characterization from a multivariate perspective: A review. Journal of Hydrology, 527: 668–678. https://doi.org/10.1016/j.jhydrol.2015.05.031

Heidrich, O., Reckien, D., Olazabal, M., Foley, A., Salvia, M., de Gregorio Hurtado, S. et al. (2016). 'National Climate Policies across Europe and Their Impacts on Cities Strategies', Journal of Environmental Management, 168(1): 36-45. https://doi.org/10.1016/j.jenvman.2015.11.043

Heim, R.R. (2002). A review of twentieth-century drought indices used in the United States. Bulletin of the American Meteorological Society, 83(8): 1149–1165. https://doi.org/10.1175/1520-0477(2002)083<1149:AROTDI>2.3.CO;2

IPCC (2014). Climate Change 2014 Part A: Global and Sectoral Aspects. In Climate Change 2014: Impacts, Adaptation, and Vulnerability. Part A: Global and Sectoral Aspects. Contribution of Working Group II to the Fifth Assessment Report of the Intergovernmental Panel on Climate Change. Geneva, Switzerland. https://www.ipcc.ch/report/ar5/wg2/full-report-global-aspects/

Jackson, L.P. and Jevrejeva, S. (2016). A probabilistic approach to 21st century regional sea-level projections using RCP and High-end scenarios, Global and Planetary Change, 146: 179–189. https://www.sciencedirect.com/science/article/pii/S0921818116300686

Jarvis, A., Reuter, H.I., Nelson, A. and Guevara, E. (2008). Hole-filled seamless SRTM data V4. Cali, Colombia: International Centre for Tropical Agriculture (CIAT). http://srtm.csi.cgiar.org

Jenerette, G.D. and Larsen, L. (2006). A global perspective on changing sustainable urban water supplies. Global and Planetary Change, 50(3–4): 202–211. https://doi.org/10.1016/j.gloplacha.2006.01.004

Jha, A.K., Bloch, R. and Lamond, J. (2012). Cities and Flooding : A Guide to Integrated Urban Flood Risk Management for the 21st Century. Washington, DC: World Bank Group. https://doi.org/10.1596/978-0-8213-8866-2

Jones, E., Qadir, M., van Vliet, M.T.H., Smakhtin, V. and Kang, S. mu. (2019). The state of desalination and brine production: A global outlook. Science of the Total Environment, 657: 1343–1356. https://doi.org/10.1016/j.scitotenv.2018.12.076

Jongman, B., Ward, P.J. and Aerts, J.C.J.H. (2012). Global exposure to river and coastal flooding: Long term trends and changes. Global Environmental Change, 22(4): 823–835. https://doi.org/10.1016/j.gloenvcha.2012.07.004

Jongman, B., Winsemius, H.C., Aerts, J.C.J.H., Coughlan De Perez, E., Van Aalst, M.K., Kron, W. and Ward, P.J. (2015). Declining vulnerability to river floods and the global benefits of adaptation. Proceedings of the National Academy of Sciences of the United States of America, 112(18): E2271–E2280. https://doi.org/10.1073/pnas.1414439112

Komuscu, A.U. (1999). Using the SPI to Analyze Spatial and Temporal Patterns of Drought in Turkey Using the SPI to Analyze Spatial and Temporal Patterns of Drought in Turkey. Drought Network News, 11(1), 6–13.

Lackstrom, K., Brennan, A., Ferguson, D., Crimmins, M. and Darby, L. (2013). The Missing Piece: Drought Impacts Monitoring Report from a Workshop in Tucson, AZ, March 5-6, 2013. Drought Mitigation Center Faculty Publications, 112.

Le Bars, D., Drijfhout, S. and de Vries, H. (2017). A high-end sea level rise probabilistic projection including rapid Antarctic ice sheet mass loss. Environmental Research Letters, 12(4): 044013. https://iopscience.iop.org/article/10.1088/1748-9326/aa6512

McDonald, R.I. and Shemie, D. (2014). Urban Water Blueprint: Mapping conservation solutions to the global water challenge. Washington, DC: The Nature Conservancy.

McDonald, R.I., Weber, K.F., Padowskic, J., Boucher, T. and Shemie, D. (2016). Estimating watershed degradation over the last century and its impact on water-treatment costs for the world's large cities. Proceedings of the National Academy of Sciences of the United States of America, 113(32): 9117–9122. https://doi.org/10.1073/pnas.1605354113

McDonald, R.I., Weber, K., Padowski, J., Flörke, M., Schneider, C., Green, P.A. et al. (2014). Water on an urban planet: Urbanization and the reach of urban water infrastructure. Global Environmental Change, 27(1): 96–105. https://doi.org/10.1016/j.gloenvcha.2014.04.022

Mechler, R. and Bouwer, L.M. (2015). Understanding trends and projections of disaster losses and climate change: is vulnerability the missing link? Climatic Change, 133(1): 23–35. https://doi.org/10.1007/s10584-014-1141-0

Mishra, A.K. and Singh, V.P. (2010). Review paper A review of drought concepts. Journal of Hydrology, 391(1–2): 202–216. https://doi.org/10.1016/j.jhydrol.2010.07.012

Muis, S., Verlaan, M., Winsemius, H., Aerts, J.C.J.H. and Ward, P.J. 2016. A global reanalysis of storm surges and extreme sea levels. Nature Communications, 7: 11969. https://www.nature.com/articles/ncomms11969

Muis, S., Apecechea, M.I., Dullaart, J., de Lima Rego, J., Skovgaard Madsen, K., Su, J., Yan, K. and Verlaan, M. 2020. A High-Resolution Global Dataset of Extreme Sea Levels, Tides, and Storm Surges, Including Future Projections. Frontiers in Marine Science, 29 April 2020. https://www.frontiersin.org/articles/10.3389/fmars.2020.00263/full

Naumann, G., Cammalleri, C., Mentaschi, L. and Feyen, L. (2021). Increased economic drought impacts in Europe with anthropogenic warming. Nature Climate Change, 11(6): 485–491. https://doi.org/10.1038/s41558-021-01044-3

Pedro-Monzonís, M., Solera, A., Ferrer, J., Estrela, T. and Paredes-Arquiola, J. (2015). A review of water scarcity and drought indexes in water resources planning and management. 527: 482–493. https://doi.org/10.1016/j.jhydrol.2015.05.003

Pokhrel, Y., Felfelani, F., Satoh, Y., Boulange, J., Burek, P., Gädeke, A. et al. (2021). Global terrestrial water storage and drought severity under climate change. Nature Climate Change, 11: 226–233. https://doi.org/10.1038/s41558-020-00972-w

Quesnel, K.J., Ajami, N. and Marx, A. (2019). Shifting landscapes: Decoupled urban irrigation and greenness patterns during severe drought. Environmental Research Letters, 14(6). https://doi.org/10.1088/1748-9326/ab20d4

Rigaud, K.K., de Sherbinin, A., Jones, B., Bergmann, J., Clement, V., Ober, K. et al. (2018) Groundswell: Preparing for Internal Climate Migration. Washington, DC: World Bank. https://openknowledge.worldbank.org/handle/10986/29461

Rosegrant, W.R., Cai, X. and Cline, S.A. (2002). Global Water Outlook to 2025 Averting an Impending Crisis. Washington, DC: International Food Policy Research Institute.

Saravanane, R., Ranade, V.V., Bhandari, V.M. and Seshagiri Rao, A. (2014). Urban Wastewater Treatment for Recycling and Reuse in Industrial Applications: Indian Scenario. In Industrial Wastewater Treatment, Recycling and Reuse. Elsevier Ltd. https://doi.org/10.1016/B978-0-08-099968-5.00007-6

Schumann, G.J.-P. and Bates, P.D. (2018). The Need for a High-Accuracy, Open-Access Global DEM. Frontiers in Earth Science, 6: 1–5. https://doi.org/10.3389/feart.2018.00225

Scussolini, P., Aerts, J.C.J.H., Jongman, B., Bouwer, L.M., Winsemius, H.C., De Moel, H. and Ward, P.J. (2016). FLOPROS: an evolving global database of flood protection standards. Natural Hazards and Earth System Sciences, 16(5): 1049–1061. https://doi.org/10.5194/nhess-16-1049-2016

Shughrue, C. and Seto, K.C. (2018). Systemic vulnerabilities of the global urban-industrial network to hazards. Climatic Change, 151(2): 173–187. https://doi.org/10.1007/s10584-018-2293-0

Stahl, K., Kohn, I., Blauhut, V., Urquijo, J., De Stefano, L., Acácio, V. et al. (2016). Impacts of European drought events: Insights from an international database of text-based reports. Natural Hazards and Earth System Sciences, 16(3): 801–819. https://doi.org/10.5194/nhess-16-801-2016

Straatsma, M., Droogers, P., Hunink, J., Berendrecht, W., Buitink, J., Buytaert, W. et al. (2020). Global to regional scale evaluation of adaptation measures to reduce the future water gap. Environmental Modelling and Software, 124: 104578. https://doi.org/10.1016/j.envsoft.2019.104578

Sutanudjaja, E.H., Van Beek, R., Wanders, N., Wada, Y., Bosmans, J.H.C., Drost, N. et al. (2018). PCR-GLOBWB 2: A 5 arcmin global hydrological and water resources model. Geoscientific Model Development, 11(6): 2429–2453. https://doi.org/10.5194/gmd-11-2429-2018

Szali ska, W., Otop, I. and Tokarczyk, T. (2018). Urban drought. E3S Web of Conferences, 45:1–8. https://doi.org/10.1051/e3sconf/20184500095

Tiggeloven, T., De Moel, H., Winsemius, H. C., Eilander, D., Erkens, G., Gebremedhin, E. et al. (2020). Global-scale benefit-cost analysis of coastal flood adaptation to different flood risk drivers using structural measures. Natural Hazards and Earth System Sciences, 20(4): 1025–1044. https://doi.org/10.5194/nhess-20-1025-2020

UCCRN (2018). The future we don't want. How Climate Change Could Impact the World's Greatest Cities. A collaboration between C40 Cities, Global Covenant of Mayors, Acclimatise, and the Urban Climate Change Research Network (UCCRN). New York, Columbia University. https://www.c40.org/what-we-do/scaling-up-climate-action/adaptation-water/the-future-we-dont-want/

UNDESA (2019). World Urbanization Prospects: The 2018 Revision. In Demographic Research. New York: United Nations Department of Economic and Social Affairs. https://population.un.org/wup/publications/Files/WUP2018-Report.pdf

UN-Habitat (n.d.). What is a City? Nairobi. https://doi.org/10.1215/9780822390732-002

UNDRR (n.d.). 'Terminology'. Geneva, Switzerland: United Nations Office for Disaster Risk Reduction. www.undrr.org/terminology

UNDRR (2019). GAR Global Assessment Report on Disaster Risk Reduction. Geneva, Switzerland: United Nations Office for Disaster Risk Reduction (UNDRR). https://gar.undrr.org/

UNDRR and CRED (2020). An overview of the last 20 years the last 20 years. 17. Geneva, Switzerland: United Nations Office for Disaster Risk Reduction and Centre for Research on the Epidemiology of Disasters. https://www.undrr.org/publication/human-cost-disasters-overview-last-20-years-2000-2019

UNESCO (2009). The United Nations World Water Development Report 3: Water in a Changing World. Paris, France: United Nations Educational, Scientific and Cultural Organization. https://doi.org/10.1142/9781848160682_0002

UNISDR (2009). Drought Risk Reduction Framework and Practices: contributing to the implementation of the Hyogo Framework for Action. Geneva, Switzerland: United Nations International Strategy for Disaster Reduction. https://www.unisdr.org/files/11541_DroughtRiskReduction2009library.pdf

van Beek, L.P.H. & Bierkens, M.F.P. (2009). The Global Hydrological Model PCR-GLOBWB: Conceptualization, Parameterization and Verification. Utrecht, the Netherlands: Utrecht University, Department of Physical Geography. https://vanbeek.geo.uu.nl/suppinfo/vanbeekbierkens2009.pdf

Van Beek, L.P.H. Wada, Y. and Bierkens, M.F.P. (2011). Global monthly water stress: 1. Water balance and water availability. Water Resources Research, 47(7). https://doi.org/10.1029/2010WR009791

Van Huijstee, J., van Bemmel, B., Bouwman, A. and van Rijn, F. (2018). Towards an Urban Preview: Modelling future urban growth with 2UP. The Hague, the Netherlands: PBL Netherlands Environmental Assessment Agency (August issue). https://www.pbl.nl/en/publications/towards-an-urban-preview#:~:text=Towards%20an%20Urban%20Preview%20(2UP)&text=As%20the%20global%20population%20is,urban%20population%20and%20urban%20expansion

Van Loon, A. F. and Van Lanen, H.A.J. (2012). A process-based typology of hydrological drought. Hydrology and Earth System Sciences, 16(7): 1915–1946. https://doi.org/10.5194/hess-16-1915-2012

Van Loon, A.F., Gleeson, T., Clark, J., Van Dijk, A.I.J.M., Stahl, K., Hannaford, J. et al. (2016). Drought in the Anthropocene. Nature Geoscience, 9(2): 89–91. https://doi.org/10.1038/ngeo2646

Veldkamp, I.E.T. and Ward, P.J. (2015). Global Earth Observation for integrated water resource assessment Report on the current state-of-the-art Water Resources Reanalysis. March. Brussels: European Commission. https://cordis.europa.eu/project/id/603608/reporting

Wada, Y., Flörke, M., Hanasaki, N., Eisner, S., Fischer, G., Tramberend, S. et al. (2016). Modeling global water use for the 21st century: The Water Futures and Solutions (WFaS) initiative and its approaches. Geoscientific Model Development, 9(1): 175–222. https://doi.org/10.5194/gmd-9-175-2016

Ward, P.J., Strzepek, K.M., Pauw, W.P., Brander, L.M., Hughes, G.A. and Aerts, J.C.J.H. (2010a). Partial costs of global climate change adaptation for the supply of raw industrial and municipal water: A methodology and application. Environmental Research Letters, 5(4). https://doi.org/10.1088/1748-9326/5/4/044011

Ward, P.J., Pauw, P., Brander, L.M., Aerts, J.C.J.H. and Strzepek, K.M. (2010b). Costs of Adaptation Related to Industrial and Municipal Water Supply and Riverine Flood Protection. Climate Change Discussion Paper No. 6. Washington, DC: World Bank. https://assets.publishing.service.gov.uk/media/57a08b20e5274a27b2000987/DCCDP_6Riverine.pdf

Ward, P.J., Jongman, B., Salamon, P., Simpson, A., Bates, P., De Groeve, T. et al. (2015). Usefulness and limitations of global flood risk models. Nature Climate Change, 5(8): 712–715. https://doi.org/10.1038/nclimate2742

Ward, P.J., Jongman, B., Aerts, J.C.J.H., Bates, P.D., Botzen, W.J.W., Diaz Loaiza, A. et al. (2017). A global framework for future costs and benefits of river-flood protection in urban areas. Nature Climate Change, 7(9): 642–646. https://doi.org/10.1038/nclimate3350

Ward, P. J., Blauhut, V., Bloemendaal, N., Daniell, E. J., De Ruiter, C. M., Duncan et al. (2020a). Review article: Natural hazard risk assessments at the global scale. Natural Hazards and Earth System Sciences, 20(4): 1069–1096. https://doi.org/10.5194/nhess-20-1069-2020

Ward, P.J., Winsemius, H.C., Kuzma, S., Bierkens, M.F.P., Bouwman, A., de Moel, H. et al. (2020b). Aqueduct Floods Methodology. Technical Note. Washington, DC: World Resources Institute. www.wri.org/publication/aqueduct-floods-methodology

Weedon, G.P., Gomes, S., Viterbo, P., Shuttleworth, W.J., Blyth, E., Österle, H., Adam, J.C., Bellouin, N., Boucher, O. and Best, M. (2011). Creation of the WATCH forcing data and its use to assess global and regional reference crop evaporation over land during the twentieth century. Journal of Hydrometeorology, 12(5): 823–848. https://doi.org/10.1175/2011JHM1369.1

Wilhite, D.A. and Glantz, M.H. (1985). Understanding: the drought phenomenon: the role of definitions. Water International, 10(3): 111–120. https://digitalcommons.unl.edu/cgi/viewcontent.cgi?article=1019&context=droughtfacpub

Wilhite, D.A., Svoboda, M.D. and Hayes, M.J. (2007). Understanding the complex impacts of drought: A key to enhancing drought mitigation and preparedness. Water Resources Management, 21(5): 763–774. https://doi.org/10.1007/s11269-006-9076-5

Winsemius, H.C., Van Beek, L.P.H., Jongman, B., Ward, P.J. and Bouwman, A. (2013). A framework for global river flood risk assessments. Hydrology and Earth System Sciences, 17(5): 1871–1892. https://doi.org/10.5194/hess-17-1871-2013

Winsemius, H.C., Ward, P.J., Gayton, I., ten Veldhuis, M.C., Meijer, D.H. and Iliffe, M. (2019). Commentary: The need for a high-accuracy, open-access global DEM. Frontiers in Earth Science, 7: 1–4. https://doi.org/10.3389/feart.2019.00033

Yamazaki, D., Kanae, S., Kim, H. and Oki, T. (2011) 'A physically based description of floodplain inundation dynamics in a global river routing model', Water Resources Research, 47(4). https://agupubs.onlinelibrary.wiley.com/doi/10.1029/2010WR009726

Zhang, X., Chen, N., Sheng, H., Ip, C., Yang, L., Chen, Y. et al. (2019). Urban drought challenge to 2030 sustainable development goals. Science of the Total Environment, 693: 133536. https://doi.org/10.1016/j.scitotenv.2019.07.342

Zhou, Y. and Tol, R.S.J. (2005). Evaluating the costs of desalination and water transport. Water Resources Research, 41(3): 1–10. https://doi.org/10.1029/2004WR003749

**Authors**

**C40**

Neuni Farhad

Snigdha Garg

Rachel Huxley

**Institute for Environmental Studies (IVM)**

Tristian Stolte

Hans De Moel

Philip Ward

**Climate Adaptation Service (CAS)**

Felix van Veldhoven

Eva Boon

Daniel Staal

**Acknowledgements**

**With special thanks to**

**C40**

Amanda Ikert

Lykke Leonardsen

Rebecca Ilunga

**Expert Advisors**

Christian Schou

Cedric Macleod

Daniela Bemfica

Oriana Romano

Juliette Lassman

Marcelo Gomez Miguez

Guy Pegram

John Matthews

**Cities**

New York City

Greater London Authority

Rio de Janeiro

Durban (eThekwini)

Rotterdam

Houston

**Designed by**

Erin Dwi Azmi

**Edited by**

Poilin Breathnach, Erin Editorial